CHALMERS
UNIVERSITY OF TECHNOLOGY

Predictive Diesel Combustion Using DI-Pulse in GT-Power

Master's thesis in Automotive engineering

VIJAYAKRISHNAN VENKATESHMOHAN
MASOOM KUMAR

Department of Applied Mechanics
CHALMERS UNIVERSITY OF TECHNOLOGY
Gothenburg, Sweden 2015

MASTER'S THESIS IN AUTOMOTIVE ENGINEERING

Predictive Diesel Combustion Using DI-Pulse in GT-Power

VIIJAYAKRISHNAN VENKATESHMOHAN

MASOOM KUMAR

Department of Applied Mechanics
Division of Combustion
CHALMERS UNIVERSITY OF TECHNOLOGY
Göteborg, Sweden 2015

Predictive Diesel Combustion Using DI-Pulse in GT-Power

VIJAYAKRISHNAN VENKATESHMOHAN
MASOOM KUMAR

Master’s Thesis 2015:88
ISSN 1652-8557
Department of Applied Mechanics
Division of Combustion
Chalmers University of Technology
SE-412 96 Göteborg
Sweden
Telephone: + 46 (0)31-772 1000

Cover:
Combustion in a Diesel engine. Painted by Pooja Umeshkumar

Chalmers reproservice
Göteborg, Sweden 2015

PREDICTIVE DIESEL COMBUSTION USING DI PULSE IN GT-POWER
Master’s thesis in Automotive Engineering
VIJAYAKRISHNAN VENKATESHMOHAN
MASOOM KUMAR
Department of Applied Mechanics
Division of Combustion
Chalmers University of Technology

ABSTRACT

Rising fuel prices and stricter emission regulations have put a great demand on developing new engines with high fuel efficiency and low emissions. This has led to the development of several new concepts such as different types of EGR, variable valve timing, different injection strategies, turbulence enhancement techniques, etc.

Virtual simulations, particularly 1D simulation tools for gas exchange have played a critical role in the last decade to reduce the lead time for the development of these new concepts. These simulation tools employ a 0D combustion model. However, one of their major limitation is the use of a non-predictive or fixed burn rate combustion model. With this kind of model it is not possible to evaluate the above mentioned concepts with reliability. In order to overcome this problem major tool developers such as Gamma Technologies have developed a predictive combustion model, which can predict the combustion rate based on the in cylinder conditions. But these models can provide reliable results only if they are well calibrated against test data.

The aim of this thesis was to calibrate a predictive combustion model for a Diesel engine in GT-Power using the DI-Pulse combustion object. The performance of the fully calibrated model was evaluated by analysing its capability to predict key operating parameters such as IMEP, CA at 50% burn, peak pressure and NO_x .

In order to calibrate the model, data was collected by conducting tests in a single cylinder test cell and was subsequently validated thoroughly before using it for calibration.

It was concluded that the model was able to predict the key operating parameters mentioned previously within the suggested thresholds except for NO_x at low loads and low speeds and peak pressure at high loads and high speeds.

Key words: Diesel combustion, Predictive combustion model, Calibration, Three Pressure Analysis, DI-Pulse, GT-Power.

TABLE OF CONTENTS

PREFACE

The thesis focuses on calibrating a predictive combustion model in GT-Power for a direct injected Diesel engine. The work was carried out at Volvo Car Corporation (VCC) from January 2015 to June 2015. We would like to thank Mattias Ljungqvist, Group manager of Engine CAE Fluids at VCC for giving us an opportunity to carry out this thesis and support us in every possible way. We would like to thank our examiner Sven B Andersson at the Department of Applied Mechanics, Chalmers for providing us the support, motivation and constructive feedback throughout the thesis. We would like to thank our supervisor Björn Jonsson at VCC for providing his guidance and recommendations to the thesis. Our special thanks to Jian Zhu at VCC who provided immense support with the technical aspects of the thesis. Further we would also like to thank Arjan Helmantel and Fredrik Holst at the single cylinder test rig and Gunnar Olsson and Eric Ött at the injector flow rig in VCC for helping us with the collection of test data. This thesis would not have been successful without the help of Robert Wang at Gamma Technologies who supported us with every question we had regarding the software and the model. Finally, we would like to thank the supplier, DENSO for providing us with the GT-Suite injector model.

Göteborg, October 2015

VIJAYAKRISHNAN VENKATESHMOHAN, MASOOM KUMAR

REPRESENTATIONS

Symbol	Unit	Description
Cent		Calibration constant - Entrainment multiplier.
C_{ign}	-	Calibration constant for ignition delay
C_{pm}	-	Calibration constant for pre-mixed phase
Q_{ch}	J	Chemical Energy released
C_D		Coefficient of discharge across the injector nozzle
R_c	-	Compression ratio
Q_C	J	Convective heat transfer
V_{cy}	m3	Cylinder volume
ρ_g	kg/m3	Density of gas
ρ_l	kg/m3	Density of liquid fuel
d_n	m	Diameter of injector nozzle
d_d	m	Diameter of the droplet
C_{df}	-	Diffusion combustion calibration constant
h_a	J/kg	Enthalpy of the air
$h_{f,i}$	J/kg	Enthalpy of the fuel injected
h_f	J/kg	Enthalpy of the fuel mass
h_i	J/kg	Enthalpy of the injected fuel
H_{vd}	kJ/kg	Enthalpy of vaporization of liquid droplet
Q_{htr}	J	Heat transfer across cylinder wall
Q_u	J	Heat transfer across the unburnt zone boundary
Q_e	J	Heat transfer due to phase change of the droplet
Q_b	J	Heat transfer to across the system boundary
t_{ign}	s	Ignition delay
u_{inj}	m/s	Injection velocity
p	Pa	Instantaneous pressure in the cylinder
V	m^3	Instantaneous volume of the cylinder
U	J	Internal energy of the system
λ	-	Lambda of the air-fuel mixture
m_a	kg	Mass of air
m	kg	Mass of entrained air-fuel mixture
$m_{f.i}$	kg	Mass of fuel injected
m_{inj}	Kg	Mass of injected fuel
m_b	kg	Mass of the burnt zone
m_d	kg	Mass of the droplet

m_f	kg	Mass of the fuel flowing across system boundary
m_u	kg	Mass of unburnt zone
m_i	kg	Mass transfer across system boundary
W	J	Net work done on the system
S	m	Penetration distance of the jet
ΔP	Pa	Pressure differential between upstream and downstream of the
k	-	Rate constant for the reaction
γ		Ratio of specific heat C_p/C_v
c_v	J/kg-K	Specific heat capacity of the mixture
c_{pd}	J/kg-K	Specific heat constant of the droplet
γ	-	Specific heat ratio
u_u	J/kg	Specific internal energy of the unburnt zone
u_b	J/kg	Specific internal energy of the unburnt zone
T	K	Temperature of the cylinder contents
T_d	K	Temperature of the droplet
T_g	K	Temperature of the gas
η_{th}	-	Thermal efficiency
t_b	s	Time to breakup of the spray into droplets
Q_{tot}	J	Total heat transfer across the system boundary
V_b	m3	Volume of the burnt zone
V_u	m3	Volume of the unburnt zone

ABBREVIATIONS

AEAP	Average Exhaust Absolute Pressure
BDC	Bottom Dead Centre
BMEP	Brake mean effective pressure
CA50%	Crank Angle for 50% Fuel Burn
CPOA	Cylinder Pressure Only Analysis
CR	Compression Ratio
DOE	Design of Experiments
EGR	Exhaust Gas Recirculation
EOI	End of Injection
EVC	Exhaust Valve closing
EVO	Exhaust Valve Opening
IMEP	Indicated mean effective pressure
IRM	Injection Rate Map
IVC	Intake Valve Closing
LHV	Latent Heat Value
RDE	Real Drive Emissions
RLT	Result
RSC	Rig Stability Check
SOI	Start of Injection
TDC	Top Dead Centre
TPA	Three Pressure Analysis

1 INTRODUCTION

This section gives a brief introduction about the background of the thesis and states the aim, objective, limitation and content of the thesis.

1.1 BACKGROUND

Rising fuel prices and stricter emission regulations have put a great demand on developing new engines with high fuel efficiency and low emissions. This has led to the development of several new concepts such as different types of EGR, variable valve timing, different injection strategies, turbulence enhancement techniques, etc.

Virtual simulations, particularly 1D simulation tools for gas exchange have played a critical role in the last decade to reduce the lead time for the development of these new concepts. These simulation tools employ a 0D combustion model. However one of their major limitation is the use of a non-predictive or fixed burn rate combustion model. With this kind of model it is not possible to evaluate the above mentioned concepts with reliability. In order to overcome this problem major tool developers such as Gamma Technologies have developed a predictive combustion model, which can predict the combustion rate based on the in cylinder conditions. But these models can provide reliable results only if they are well calibrated against the test data.

1.2 AIM

The aim of the project is to calibrate a predictive combustion model for a DI Diesel engine in GT-Power using the DI-Pulse combustion object. The fully calibrated model should be able to predict the IMEP, CA at 50% burn, peak pressure and NO_x within the suggested thresholds.

1.3 OBJECTIVE

- Perform a literature survey to gain an understanding on the different combustion models available for a DI Diesel engine.
- Validate the injector model obtained from the supplier against test data obtained from injector flow rig.
- Collect data from the engine test cell for 28 operating points based on the RDE driving cycle.
- Perform Three Pressure Analysis (TPA) and Cylinder Pressure Only Analysis (CPOA) on the data collected to validate it.
- Calibrate the model against 25 points and obtain the multipliers for the combustion model.
- Validate the combustion model against 3 points.
- Calibrate the emission model for NO_x and validate it against the test data.

1.4 LIMITATION

The general recommendation from Gamma Technologies is to calibrate the model against 200 points spread across the entire speed and load map. However, for this project due to the time constraint only 28 points have been selected with most of them covering low to mid speed and low to mid load region where the engine is most likely to operate in for most of the time.

Also, due to time limitation the validation of the model would be performed against only 3 points. The optimal way would have been to perform a sensitivity analysis by running sweeps of EGR and injection timing at different speed and load points.

The final calibration results will be based on only a closed volume analysis model in which, the cylinder, injector and crank train are isolated. A fully integrated engine model having intake and exhaust subsystems will not be utilized due to time constraint.

1.5 CONTENTS OF THE THESIS

This report is primarily divided into five parts. Part 1 covers the literature study about Diesel engine basics and Diesel combustion modelling in GT-Power. Part 2 describes the methodology followed in the thesis. Part 3 includes the results and discussions. Part 4 concludes the findings. Part 5 provides the final recommendation and future work to be done.

2 DIESEL COMBUSTION THEORY

This section is divided into four main parts. The first part gives brief information about working of Diesel engines including Diesel combustion, emission formation and other common sub systems such as exhaust gas recirculation and fuel injection systems. The second part describes about GT-Power and modelling combustion in it. The third section describes briefly about validation of data collected from a single cylinder test cell. The final section provides information about burn rate analysis using the test data in GT-Power.

2.1 DIESEL ENGINE BASICS

The working of Diesel/Compression ignition (CI) engine is fundamentally different from a spark ignition (SI) engine. In a SI engine a spark ignites the combustible mixture. The combustion is homogenous and ideally takes place at constant volume. In CI engines fuel is injected late in the compression stroke, which mixes with air and auto ignites under high pressure and temperature. Hence the combustion is heterogeneous and takes place at constant pressure (Sundararajan, et al., 2015). Theoretically SI engines have a higher thermal efficiency compared to CI engines for a given compression ratio as shown in Eq. 2.1 and 2.2 (Taylor, 1966). However one of the inherent disadvantages of a SI engine is the tendency to knock, which limits the compression ratio and subsequently the efficiency. In a CI engine there is no risk of knock, hence they can operate at a significantly higher compression ratio leading to better efficiency (Heywood, 1988). CI engines also benefit from the stratified combustion mode, i.e. fuel is injected at the end of the compression stroke and burns predominantly as a diffusion combustion. This enables lean burn, which improves the thermal efficiency. It also avoids the need of a throttle, which reduces the pumping losses. These factors make a CI engine upto 30% more efficient than a SI engine (Cars Direct, 2015).

$$\text{Thermal efficiency of SI engine} \quad \eta_{th} = 1 - \frac{1}{R_c^{\gamma-1}} \tag{2.1}$$

$$\text{Thermal efficiency of CI engine} \quad \eta_{th} = 1 - \frac{R_c{}^{1-\gamma}\left(R_c^{\gamma}-1\right)}{\gamma(R_c-1)} \tag{2.2}$$

However Diesel engines also have some important demerits. Due to the increased complexity of the engine, the manufacturing cost is higher. Due to the lean burn mode, a three way catalyst is not effective. This drives up the complexity of the after treatment system and subsequently increasing the cost and emissions (Heywood, 1988).

2.1.1 COMBUSTION IN DIESEL ENGINES

The combustion in a Diesel engine can be divided into four distinct phases namely (Rajput, 2007), as shown in figure 2.1

I. Ignition delay
II. Premixed combustion
III. Mixing controlled combustion
IV. After burn

These phases are explained in detail below.

i. Ignition delay

Ignition delay period is defined as the time taken between start of injection and start of combustion. It can be classified into two parts (Rajput, 2007).   .

- **Physical delay**
  Physical delay is defined as the time taken between start of fuel injection and attainment of chemical reaction conditions. During this period the fuel is atomized, vaporized and the mixture is raised in temperature.

- **Chemical delay**
  Chemical delay is defined as the time taken between attainment of chemical reaction conditions and ignition. During this period the reaction starts slowly and then accelerates until ignition.

Ignition delay has a great influence on combustion. Higher the delay period, more rapid and higher the pressure rise during the premixed combustion phase leading to increased noise and rough running of the engine. This is the primary reason for noisy operation of Diesel engines compared to gasoline engines. Ignition delay is influenced by several factors.

- **Temperature at the time of injection**: Higher the temperature, lower the ignition delay.
- **Relative velocity between fuel injection and air turbulence**: Higher the relative velocity, better the mixing, hence lower the ignition delay.
- **Compression Ratio (CR)**: Higher the CR, higher the air temperature and density, hence lower the ignition delay.
- **Injection timing**: The effect of injection timing is described in detail in section 2.1.6.
- **Fuel properties**: Fuel properties such as auto ignition temperature, volatility, latent heat, etc. can have an effect on ignition delay.

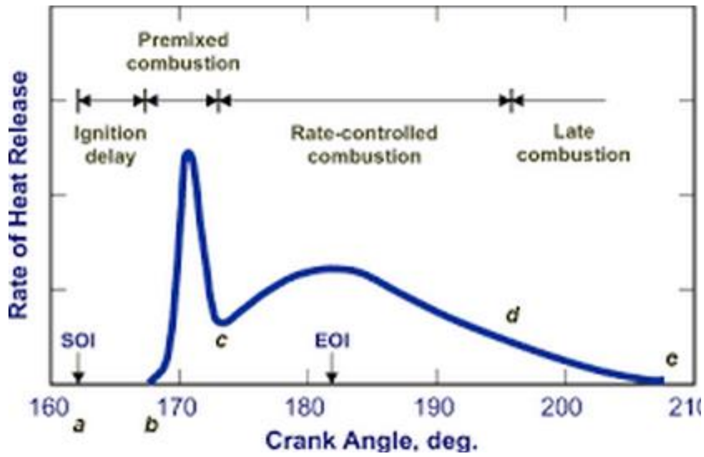

Figure 2.1: Phases of Diesel combustion (Heywood, 1988)

ii. Premixed combustion

This phase is also known as the rapid/uncontrolled combustion, since the fuel is mixed with air during the delay period and leads to rapid pressure rise. The rate of pressure rise depends upon the amount of fuel present at the end of the delay period, degree of turbulence, fineness of atomization and spray pattern (Rajput, 2007).

iii. Mixing controlled combustion

At the end of the premixed phase of combustion the temperature and pressure is very high and any fuel that enters after that burns almost instantaneously. The rate of combustion can be easily controlled by the rate of injection (Rajput, 2007).

iv. After burn

The combustion continues even after the fuel injection is over due to the poor distribution of fuel particles. Not much useful work can be extracted from this phase as the piston has already completed part of the expansion stroke (Rajput, 2007).

2.1.2 DIESEL EMISSIONS

The two major emissions from a Diesel engine are soot and oxides of nitrogen (NO_x) (Heywood, 1988). The formation of these two are explained in detail below.

➢ Oxides of Nitrogen (NO_x)

The NO_x formation is governed by the extended Zeldovich mechanism shown in reaction below. The two major factors which aid the formation of NO_x is the availability of excess air and high temperature. Since Diesel engines operate under lean conditions, NO_x is significantly higher compared to SI engines, which operate close to stoichiometry (Heywood, 1988).

NO_x is harmful as they react with water to form nitric acid leading to acid rain (Sharma,2014). NO_x particles are also very fine and can penetrate into the lungs leading to respiratory problems (Environment Protection Agency, USA, 2014).

$$N_2 + O \Longleftrightarrow NO + N$$

$$N + O_2 \Longleftrightarrow NO + O$$

$$N + OH \Longleftrightarrow NO + H$$

➢ Soot

Soot is a result of incomplete combustion of fuel. SI engines burn homogenously, hence the formation of soot is small. However, in Diesel engines due to the heterogeneous combustion, fuel rich pockets are formed which breakdown eventually leading to the formation of soot (Heywood, 1988) as shown in figure 2.2 (Heywood, 1988). High temperatures towards the end of combustion help burn some of the soot particles before they can escape to the environment (Southernfs, 2015).

The details of the mechanism leading to the formation of soot are not well known but it is a well-defined fact that the primary variables affecting soot formation are pressure, temperature and equivalence ratio (Perini et al., 2015). Hence a more simplified empirical model is used in calculations based on the formation – oxidation model (Wang, 2014). This model is shown with the help of the Eq. 2.3 (Jung and Assanis, 2001).

$$\frac{dm_s}{dt} = \frac{dm_f}{dt} - \frac{dm_o}{dt} \quad (2.3)$$

Where $\frac{dm_s}{dt}$ is the net rate of formation of soot, $\frac{dm_f}{dt}$ is the rate of formation of the soot in the fuel rich spray core and $\frac{dm_o}{dt}$ is the rate of oxidation of the soot

Not only is soot harmful for the environment, but can also pose a major threat to the engine. Most of the soot escapes through the exhaust, while small amounts leak past the piston and mix with the lubricants. As the quantity of soot in the oil increases, its viscosity increases leading to increased friction and engine wear.

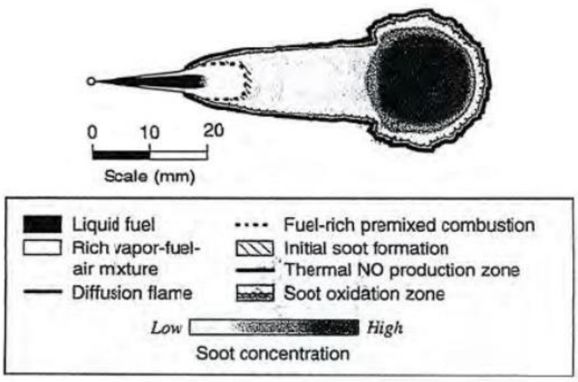

Figure 2.2: Concentration of soot in a diffusion flame (Dec, 1997)

The major problem in a Diesel engine is the contradicting conditions which help reduce NOx and soot emissions. High temperatures help burn the soot particles however high temperature would lead to increased NOx formation. Lean mixtures help reduce soot formation but increase NOx due to the excess availability of O2 (Zhao, 2010). This contradiction is shown in figure 2.3. However extremely lean mixtures reduce NOx formation due to the reduction in temperature but they also reduce the power output and in extreme cases makes the combustion erratic and leads to increase in fuel consumption (Heywood, 1988).

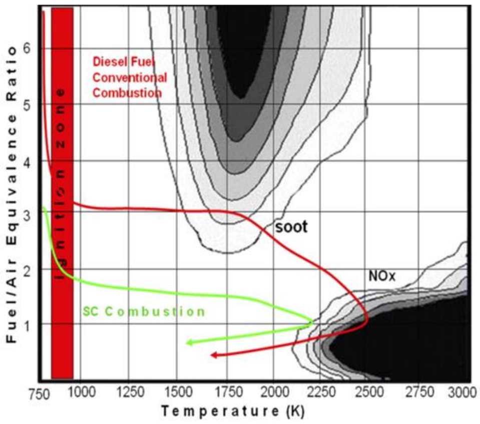

Figure 2.3: Soot and NOx formation against temperature and equivalence ratio (George Anitescu, 2012)

2.1.3 EXHAUST GAS RECIRCULATION

As explained in section 2.1.2, one of the major factors for NOx formation is high temperature in the combustion chamber and the availability of O_2. The temperature can be brought down by recirculating the exhaust gases. Exhaust Gas Recirculation (EGR) was first introduced in 1990's but was not seen as major breakthrough until the introduction of Euro 3 legislations which placed strict demand on the NO_x level (Khair et al., 2014). In today's Diesel engines EGR have become common.

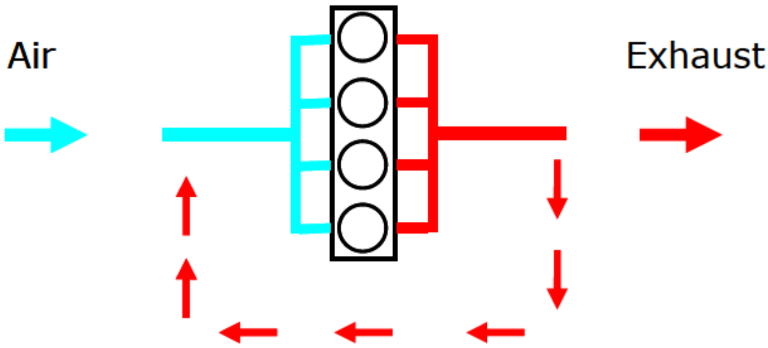

Figure 2.4: Schematic diagram of EGR system (Reifarth, 2010)

EGR helps reduce the temperature primarily due to two reasons (Reifarth, 2010).

1. Fuel molecules need more time to find and react with the O_2 molecules due to the presence of inert gases, this slows down the combustion rate and reduces the peak temperature.

2. Exhaust gases have a higher heat capacity compared to air which reduces the temperature rise in the cylinder.

EGR is classified into two types, internal and external EGR (Schäfer and Basshuysen, 1995). In internal EGR a portion of the exhaust gas is retained for the next cycle. The amount of internal EGR can be varied by varying the valve overlap.

In external EGR, the exhaust gas is driven back to the intake manifold through an external EGR circuit. The amount of EGR fraction can be varied by the EGR control valve. The schematic view of an external EGR is shown in figure 2.4.

2.1.4 DIESEL FUEL INJECTION SYSTEM

The fuel injection system is the heart of a Diesel engine. It is a critical system, as the combustion of a Diesel engine is purely controlled by the injection timing and quantity. Whereas in a SI engine the spark timing is critical for controlling the combustion, except for a GDI stratified engine where the injection timing also plays a critical role (Kitchen, 2015).

The most commonly used fuel system in light duty Diesel engines is the Common Rail Diesel Injection (CRDI). It consists of 2 sub-systems: Low Pressure (LP) system and High Pressure (HP) system (Kitchen, 2015) shown in figure 2.5.

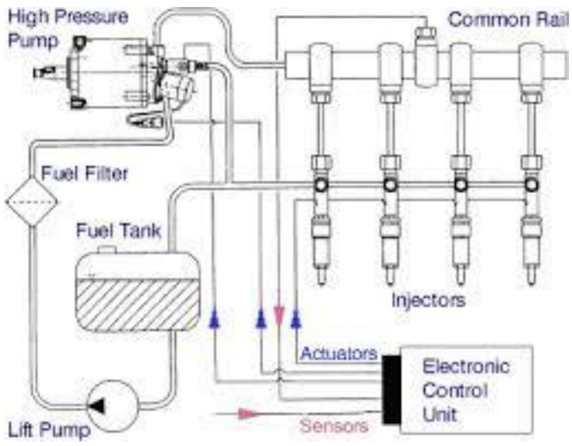

Figure 2.5: CRDI fuel system (Khair et al., 2014)

The primary goal of the low pressure system is to store, filter and deliver fuel to the high pressure fuel pump and return the excess fuel from the high pressure system back to the tank. The main components of the low pressure system are the fuel tank, filter and low pressure (LP) pump. The fuel tank stores the fuel below its flash point and also allows the fuel returned from the engine to dissipate its heat. The low-pressure pump supplies the fuel to the high-pressure (HP) pump. The filter is essential to remove impurities and also separate the water in the fuel.

The HP pump forms the interface between the two sub-systems. Diesel engines generally require very high pressure for injection compared to gasoline engines primarily due to two reasons. The fuel in a Diesel engine is injected during the end of compression stroke when the in cylinder pressure is very high and needs to be overcome. But more importantly, high pressure injection ensures higher air entrainment into the spray which facilitates faster vaporization resulting in cleaner combustion (Heywood, 1988). The HP pump is responsible for generating the high injection pressure required at each operating point.

The high pressure system consists of a common rail and an injector for each cylinder. The common rail stores the high pressure fuel and distributes it to each injector and also damps the pressure fluctuations caused by the HP pump and the injection process. The rail also has a pressure limiter valve which regulates the pressure in the rail based on the input from the ECU.

The injector ensures that the required amount of fuel is injected at the precise time. Two types of injectors are commonly used, solenoid and piezo electric. The solenoid injectors primarily consist of a solenoid, injector piston, injector needle and nozzle as shown in figure 2.6. When the solenoid is active the piston along with the needle moves up, opening the nozzle and high pressure fuel is sprayed into the cylinder. The principle of operation of piezo electric injector is similar, but has a faster response time. Hence they are preferred for high speed engines with multiple injections. The injector used for this thesis is the Denso solenoid injector capable of injection pressures up to 2500bar (Diesel Net, 2013)

The main benefit of the CRDI system over the others is that, the injection pressure is independent of the engine operating conditions. Hence a high injection pressure is even possible at low speed which improves the low speed torque of the engine. However the pressure at low speed is limited to a certain extent to avoid wall wetting which would lead to a decrease in efficiency (Kitchen, 2015).

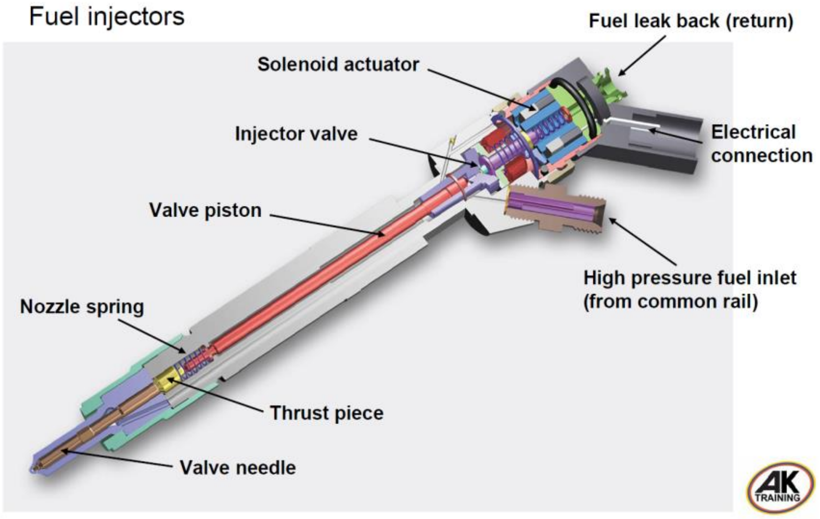

Figure 2.6: Solenoid fuel injector (Kitchen, 2015)

2.1.5. INJECTION STRATEGY IN DIESEL ENGINES.

The Diesel combustion is extremely sensitive to the injection strategy. Modern high speed Diesel engines employ multiple injections per cycle in order to reduce the emissions, noise and bsfc (Badami et al., 2002).

Multiple injections can be divided into pre, main and post injections. Pre-injections are predominantly used to reduce combustion noise and post injections help reduce soot emissions.

The major reason for noisy operation of Diesel engines compared to gasoline is due the rapid premixed combustion. The premixed combustion peak is directly related to the ignition delay (Heywood, 1988).

During pre-injection a small quantity of fuel is injected and undergoes homogenous combustion, this raises the temperature of the cylinder and reduces the ignition delay for the main injection, in turn reducing the premix combustion peak. This results in quieter operation of the engine as shown in figure 2.7. The reduced ignition delay also advances the combustion which improves the efficiency. However this leads to an increase in soot production due to longer diffusion combustion duration. The NO_x also increases due to the increase in cylinder temperature since the combustion is advanced (Badami et al., 2002).

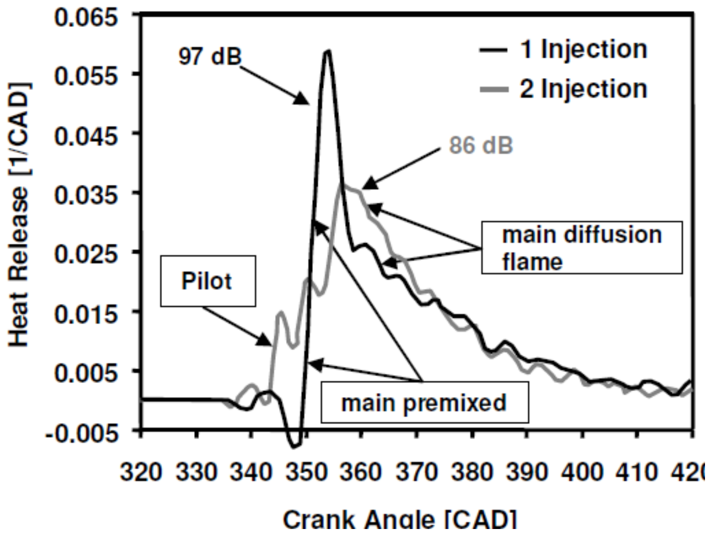

Figure 2.7: Heat release rate with and without pre injection (Asad et al. , 2008)

The timing for pre injection is critical. If the fuel is injected very early, the fuel dissipates and forms an ultra-lean mixture and doesn't burn. This increases the ignition delay leading to a higher pre-mix combustion peak compared to a single injection strategy. Very early pre injection is only used for Low Temperature Combustion (LTC) Diesel (Asad et al., 2008).

In post injections a small quantity of fuel is injected after the main injection. The main aim of this is to reduce soot emissions. The main reason for soot formation is the fuel rich zone formed in the spray during the diffusion combustion. Post injections do not directly have an effect on soot formation. However they help maintain a high temperature towards the end of combustion, which helps burn the soot formed previously (Badami et al., 2002).

Most emissions in an engine occur mainly in the warm up period, due to low temperature of the catalyst, which drastically reduces its conversion efficiency (Heywood, 1988). Post injections help increase the exhaust temperature and reduce the time taken for the catalyst to reach its optimum temperature.

Similar to pre injection, the timing is very critical for post injections as well. Very early post injections increase the soot formation. This is mainly due to the fact that the fuel is injected during the diffusion part of the main combustion which creates a cooling effect and reduces the temperature of the main combustion and increases the soot formation.

With the betterment of injector response time, manufacturers are looking to implement multiple pre and post injections to further reduce the noise and soot emissions (Badami et al., 2002).

As the number of injections increase, each injection is affected by the previous injection due to the pressure fluctuations in the fuel system. The CRDI helps damp out these fluctuations and tries to maintain a constant injection pressure (Kitchen, 2015).

The development of technologies such as, EGR, multiple turbo chargers etc. has had an impact on the injection strategy. For instance with increasing EGR, the soot increases. In order to prevent this, the injection pressure is increased for better air entrainment (Rosli, 2011).

2.2. MODELLING

This section describes briefly about the classification of combustion models and explains in detail about the combustion models for Diesel engines which are available in GT-Power. The section also briefly covers upon modelling of a Diesel fuel injection system in GT-Suite.

2.2.1. COMBUSTION MODELING

Combustion models are used for the purpose of analysis and prediction of engine performance and emission related characteristics. These models can be classified as thermodynamic and fluid dynamic in nature (Heywood, 1988). Thermodynamic models are based on energy conservation equations while the fluid dynamic models are based on the analysis of flow fields inside the engine. Each of the approaches have their own advantages and constraints which will be discussed in the following sections.

2.2.1.1. Thermodynamic based model

Thermodynamic based model are commonly of two types.

- 0-D Combustion model
- Phenomenological model

These models are described in detail below.

- **0-d Combustion model**

0D models are essentially open thermodynamic systems, used to estimate the instantaneous cylinder combustion parameters $(P, T, RoHR, etc)$ based on the conservation of energy and mass equations (Heywood, 1988), (Payri et al. , 2011). In accordance with the governing law of thermodynamic analysis, a uniform thermodynamic state and composition is assumed to exist throughout the control volume, which is invariant with respect to infinitesimal time steps over which the entire process is resolved. These models are usually based on simplifications and hence are generally used for analysis of heat release, burn rate and fuel consumption. They have limited predictive capability in terms of emission due to lack of spatial resolution (Payri et al., 2011). However, they form very good tool for parametric exploration of different engine configuration and operating conditions (Payri et al., 2011).

- **Phenomenological model**

The 0-D combustion models are simplified models used to study basic engine performance characteristics based on conservation laws as described earlier. However due to the complexity of modern Diesel engines, many input parameters such as – injection timing, number of pulses, EGR etc., affect performance and emissions. This is difficult to predict using the base 0D models (Barba et al.,2000), (Payri et al.,2011). The phenomenological models bridge the gap by modelling the underlying physical and chemical process (phenomenon) to improve the overall predictive accuracy and at the same time keep the computing time reasonable (Barba et al., 2000). Modelling the effect of spray evolution, swirl and turbulence related mixing, describing premixed and mixing controlled combustion as a function of spray kinetic energy, including ignition delay model are a few examples of the features of the phenomenological models (Barba et al.,2000), (Payri et al.,2011), (Jung and Assanis, 2001). Properly calibrated models are able to provide good predictive capability for key combustion and emission related parameters while keeping the computation time short (Barba et al.,2000), (Jung and Assanis, 2001).

.

2.2.1.2 Fluid dynamics based model

Fluid dynamic models are based on the analysis of flow fields inside the engine. The most commonly used fluid dynamic based model is the 3D CFD model, which is explained below.

- **3D CFD model**

The in-cylinder flow field greatly influences the combustion characteristics such as ignition delay, RoHR, pressure rise and pollutant formation (Colin et al., 2003). Due to the introduction of advanced injection and after-treatment techniques, new combustion chamber designs, etc. the importance of understanding mixture formation and its subsequent effect on combustion characteristics is ever more increasing. Although the phenomenological models are effective in predicting key combustion parameters, especially for homogenous mixtures, it can't be used for key engine systems development such as piston bowl design, combustion chamber design and injector spray profile (Colin et al., 2003). The 3-D CFD based models bridge this gap by allowing exploration and more detailed understanding of the critical mixture formation process (Colin et al., 2003). It does so by giving information about the average flow fields inside an engine and also the relative fluctuations about the mean (Heywood, 1988). This enables a qualitative comparison of different engine / component designs.

Several methods are employed for studying the flow fields inside an engine, all varying in computation time and prediction accuracy. It is up to the engine designers to choose the right method in order to strike a reasonable balance between computational time and prediction accuracy.

2.2.2 COMBUSTION MODELS IN GT-POWER

GT-Suite is one of the most popular engine simulation software developed by Gamma Technologies. It is predominantly a 1D simulation tool with many sub programs with their own area of expertise.

GT-Power is used to study the gas exchange and combustion simulations from an overall system perspective. The solver is based on 1D unsteady, nonlinear Navier-Stokes equation. It contains thermodynamic and phenomenological models to capture the effects of combustion, heat transfer, evaporation, turbulence, tailpipe out emissions, etc. (GTI soft, 2015).

There are two kinds of combustion models in GT-Power.

- Non predictive combustion model.
- Predictive combustion model.

2.2.2.1. Non Predictive combustion model

In a Non predictive combustion model as the name suggests the burn rate is imposed and does not depend on the in cylinder conditions to characterize the combustion and emission related parameters (GT-Suite, 2013). The major benefit of this model is fast simulation time and is useful for evaluating concepts which do not have an impact on the burn rate characteristics (GT-Suite, 2013). For example, this kind of model can be used to study the wave dynamics, boosting concepts and exhaust configurations to name a few. However it would not be accurate to study phenomenon such as EGR, injection timing, etc.

2.2.2.2 Predictive combustion model

In a predictive combustion model, the burn rate is calculated for each cycle based on the in cylinder conditions. This leads to a longer simulation time compared to the non-predictive model however, it is useful to study the concepts that have an impact on the burn rate such as different injection timings, EGR and various injection profiles (GT-Suite, 2013). In order to obtain accurate predictions, the model must be calibrated initially against test data. Phenomenological predictive combustion models make use of a concept known as zone modelling in which, the combustion is modelled to take place in single or multiple zones. These models are described below in detail.

- **Single zone model**

A single zone combustion model consists of a single, usually spherical zone wherein the injection, evaporation, mixing and subsequent burning of the fuel mass happens (Barba et al., 2000). As the mixture burns, the size of the zone increases to accommodate burnt air-fuel mixture into the zone (Barba et al., 2000). The single zone model represents the same average temperature and pressure for the entire zone (Jung and Assanis, 2001). Single-zone model is good for studying the prime combustion parameters such as burn rate, RoHR and pressure trace. However due to a lack of spatial resolution in the model, it is not efficient in studying emission related variables such as NO_x and soot (Jung and Assanis, 2001).

- **Multi zone model**

The multi zone, quasi-dimensional combustion models essentially works by dividing injected fuel packets into multiple zones, each of which is treated as an open system (Jung and Assanis, 2001). The evolution of each packet of fuel is tracked separately and predictions are made with respect to its trajectory, air-entrainment and evaporation (Heywood, 1988). Furthermore the combustion equations are solved for each zone separately which depends on temperature, pressure and equivalence ratio of each zone (GT-Suite, 2013). The advantage of multi-zone combustion is that they provide enhanced spatial resolution of the key combustion parameters inside the engine compared to single-zone model thereby enabling better prediction of performance and emission related parameters (Jung and Assanis, 2001).

2.2.3 DIESEL PREDICTIVE COMBUSTION MODEL IN GT-POWER

For Diesel engines GT-Power has two specific predictive combustion models. Namely DI-Jet and DI-Pulse. Both these models are multi zone models, however the DI-Pulse is newly developed and is expected to take lesser computation time and match or exceed the accuracy of the DI-Jet model (GT SUITE, 2013).

2.2.3.1. DI-Jet combustion model

DI-Jet combustion object encompasses a multi-zone, multi-pulse combustion model developed by Gamma Technologies for the purpose of developing predictive combustion models (GT-Suite, 2013). It is a quasi-dimensional model wherein the injected fuel is divided into a number of axial splices, each containing five radial zones. A new axial splice is generated at each time-step and the mass of fuel contained in it depends on the integral of the instantaneous injection rate over the defined time step (GT-Suite, 2013). Furthermore, the mass contained in each slice is equally divided between the five radial zones. Each zone defined above is further subdivided into subzones which contain liquid fuel, entrained vapour-air mixture and burned gas as shown in the figure 2.8.

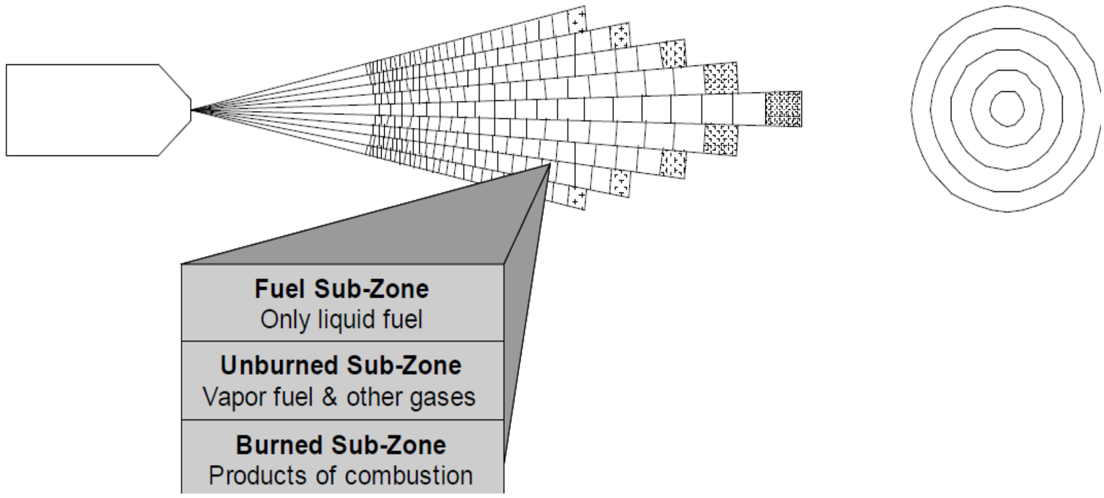

Figure 2.8: Representation of DI Jet model (Hiroyasu, 1983))

As the fuel sub-zone develops over time, it starts to entrain air and subsequent fuel mass is shifted to the unburnt sub-zone as depicted in figure 2.8. Further combustion reaction takes place based on the current temperature, pressure and mixture strength inside the unburned sub-zone and the burnt products are transferred to the burned sub-zone. NOx and soot are calculated independently for each zone, based on its conditions and later integrated to get the overall products of the combustion reaction (GT-Suite, 2013). This multi-zone approach thus yields better overall predictions about the emissions of the engine, as the emission products are resolved based on conditions existing at each zone rather than overall ensemble zone states (pressure, temperature) as in a single zone combustion model.

2.2.3.2 DI-Pulse Combustion Model

DI-Pulse is a phenomenological, multi-zone combustion model developed by Gamma Technologies to enable prediction of the in-cylinder combustion and emission associated parameters for direct injection Diesel engines with single or multi-pulse injections. The combustion rate is predicted based on pressure and temperature profile, mixture composition at IVC and injection rate profile (GT-Suite, 2013) (Wang, 2014). The average computation time is 5% more than non-predictive models and significantly faster than the DI-Jet model which it aims to replace (Wang, 2014). The model tracks each injection pulse separately and follows its evaporation, mixing with gas and the burn events. Thus it is imperative to have a high degree of accuracy while specifying the injection rate profile as an input to the model.

The DI-Pulse is a three zone combustion model. It achieves this by dividing the cylinder volume into three discrete thermodynamic zones, each with its own temperature and concentration. The first zone called the main unburnt zone contains the trapped masses at intake valve closing (IVC). The second zone called the spray unburnt zone consists of a mixture of fuel and gases which have been entrained during the injection event and the third zone called the spray burnt zone consists of the burnt combustion products (GT-Suite, 2013). Furthermore, four calibration parameters/multipliers, namely – Entrainment, Ignition delay, premixed combustion rate and diffusion combustion rate multipliers may be used to calibrate the model.

GT-Power uses different models for the different phases of combustion. The details of each phase and model used are explained below.

1. **Fuel. Injection**

   The DI-Pulse supports single/multi-pulse injection events with no limitation on the number of pulses. Each pulse is tracked separately and added to the spray unburnt zone as shown in Figure 2.9. Thus a high degree of accuracy is required for the injector model.

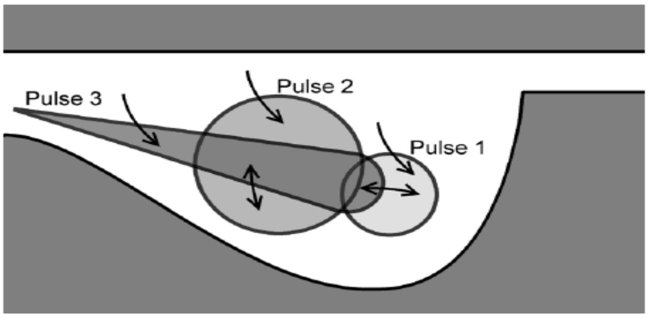

Figure 2.9 – Multi-pulse model in GT-Power (GT-Suite, 2013)

The spray penetration length ‘S’ of a pulse at a time ‘t’ after the injection event is calculated by the Eq. 2.5 before break up occurs and by Eq. 2.6 after break up occur (Wang, 2014).

$$S = u_{inj} \cdot t \cdot \left[1 - \frac{1}{16}\left(\frac{t}{t_b}\right)^8\right] ; when\ \frac{t}{t_b} \leq 1 \tag{2.4}$$

$$S = u_{inj} \cdot t_b \cdot \frac{15}{16} \cdot \left(\frac{t}{t_b}\right)^{.5} ;\ when\ \frac{t}{t_b} \geq 1 \tag{2.5}$$

where u_{inj} is the injection velocity at the injector nozzle tip, $t_b$is the time to breakup of spray into droplets.

The time to breakup of spray t_b and spray tip velocity u_{inj} is evaluated by Eq. 2.6 and Eq. 2.7 respectively.

$$t_b = \sqrt{\frac{2 \cdot \rho_l}{\rho_g}} \cdot \frac{d_n}{C_d * u_{inj}} \tag{2.6}$$

where ρ_g is the density of the gas, ρ_i is the density of the liquid fuel, C_d is the coefficient of discharge of the injector nozzle and d_n is the diameter of the nozzle.

$$u_{inj} = C_d \sqrt{\frac{2\ \Delta P}{\rho_l}} \tag{2.7}$$

Where ΔP is the pressure difference across the injector nozzle.

2. **Entrainment model**
As the fuel is injected in the cylinder environment it entrains fresh air, residual gases, and fuel from other pulses. Modeling of the entrainment is based on conservation of momentum (Wang, 2014), as shown in Eq. 2.8.

$$Initial\ spary\ momentum\ = Final\ entrainement\ mixture\ momentum$$

$$m_{inj} \cdot u_{inj} = \left(m_{inj} + m_{air-entrained}\right) \cdot u\ \ ; where\ u = \frac{dS}{dt} \tag{2.8}$$

Where m_{inj} is the initial mass of injected fuel packet, $m_{air-entrained}$ is the mass of air entrained in the packet and u is the final velocity of the entrained air-fuel mixture.

Hence, the mass of air entrained is closely dependent on injection velocity, as shown in Eq. 2.9.

$$m_{air-entrained} = \frac{m_{inj} \cdot u_{inj}}{u} \tag{2.9}$$

The rate of entrained fuel-gas mixture is modelled as shown in Eq. 2.10.

$$\frac{dm}{dt} = -\,\mathrm{C_{ent}} \cdot\ m_{inj} \cdot u_{inj} \cdot \frac{du}{dt} \tag{2.10}$$

$C_{ent}$is the entraintment multuplier can be used for calibration of the model.

3. **Evaporation**

The next step in the modeling chain is the evaporation of the fuel in the entrained mixture. A control volume is assumed around the droplet and energy balance equation is applied to it as shown in Eq. 2.11. The change in internal energy of the droplet is the sum of convective heat transfer from the hot entrained gas and the energy outflow as a result of its own evaporation (Wang, 2014).

$$m_d \cdot c_{pd} \cdot \frac{dT}{dt} = \frac{dQ_c}{dt} + \frac{dQ_e}{dt} \tag{2.11}$$

Where m_d is the mass of the droplet, c_{pd} is the specific heat capacity of the droplet.

The rate of convective heat transfer is defined by Eq. 2.12.

$$\frac{dQ_c}{dt} = h \cdot \pi \cdot d_d^2 \cdot (T_g - T_d) \tag{2.12}$$

Where d_d is the diameter of the droplet, T_g is the temperature of the entrained gases,T_d is the temperature of the droplet

The heat absorbed from the control volume due to enthalpy change is given by Eq. 2.13.

$$\frac{dQe}{dt} = -\frac{dm_d}{dt} \cdot \Delta H_{v_d} \tag{2.13}$$

Where ΔH_{vd} is the latent heat of vaporization of the droplet, $\frac{dm_d}{dt}$ is the rate of evaporation of the droplet.

4. **Ignition Delay**

It is the time between the start of injection and the start of combustion. Ignition delay is modeled separately for each pulse as a function of EGR, bulk cylinder temperature and cetane number of the fuel as shown in Eq. 2.14. The multiplier C_{ign} can be used to calibrate the model.

$$\tau_{ign} = C_{ign} \cdot \rho^{C_{ign2}} \cdot e^{\frac{C_{ign3}}{T}} \cdot f(EGR) \tag{2.14}$$

Since, the temperature and pressure constantly changes as a function of crank angle, the ignition delay is evaluated by the following relation (Livengood et al., 1955), as shown in Eq. 2.15

$$\int_{t_{soi}}^{t_{soi}+t_{id}} \frac{dt}{\tau(p, T)} = 1 \tag{2.15}$$

5. **Premixed Combustion**

   The premixed combustion takes place when the ignitable conditions are reached inside the cylinder. The air-fuel mixture developed after the elapse of the ignition delay period is used in the premixed phase of the combustion. It also depends on other factors such as temperature, air-fuel ratio, EGR fraction and the kinetic rate constant. A multiplier C_{pm} can be used to calibrate the model. The equation for modeling the premixed phase (Wang, 2014) is shown in Eq. 2.16

$$\frac{dm}{dt} = \mathrm{C_{pm}} \cdot m \cdot \left(t - t_{ign}\right) \cdot f\ (k, T, \lambda, EGR) \tag{2.16}$$

   where t is the time after injection event of the fuel packet, $\mathrm{t_{ign}}$ is the ignition delay, k is the kinetic rate constant for the combustion reaction, m is the mass of air-fuel mixture developed during the ignition delay period

6. **Diffusion combustion**

   After the premixed phase has elapsed, the reaction rate is controlled by the relative rate at which fuel and air mixture is available. The rate at which the mixture burns in diffusion controlled combustion depends on the EGR level, oxygen concentration, cylinder volume and the mass of the mixture. A diffusion combustion multiplier C_{df} can be used to calibrate the model. The equation for modeling the diffusion phase (Wang, 2014) is shown in Eq. 2.17.

$$\frac{dm}{dt} = \mathrm{C_{df}} \cdot \mathrm{m} \cdot \frac{\sqrt{k}}{\sqrt[3]{V_{cyl}}} \cdot f(EGR, [O_2]) \tag{2.17}$$

   where $\mathrm{V_{cyl}}$ is the cylinder volume, m is the mass of air-fuel mixture available at diffusion combustion stage.

2.2.4 INJECTOR MODELING

One of the most critical parameters for a reliable calibration of the combustion model is the injection rate and timing (Wang, 2014); hence they must be modelled with high accuracy. As mentioned before the main benefit of a CRDI system is the possibility to maintain a constant injection pressure at any operating point of the engine. However in reality, the engine is operated with different injection pressures to optimize for efficiency and emissions. In general at idling the pressure is minimum, while at high speeds and high loads it is maximum. In addition, the pressure in the injectors is not in steady state. Pressure fluctuations are caused due to the HP pump and the injection process. The CRDI dampens these fluctuations to a certain extent (Kitchen, 2015). Also when multiple injection strategies are employed, each injection is influenced by the pressure fluctuations of the previous injection and the effect is more significant when the gap between the two injections is very small (Zhang et al., 2015).

While modelling the fuel system in GT-Suite it is essential to take these pressure fluctuations into account. To do this, the entire fuel system particularly the high pressure components must be modelled with high accuracy. However this increases the complexity of the model and the simulation time. In general the HP pump and rail models are simplified and only the injector is modelled in detail (Ozama, 2014) but this may lead to inaccuracies in the system.

2.3 TEST CELL DATA ANALYSIS

The calibration accuracy of the model strongly depends on the accuracy of the test cell data obtained (Wang, 2014).

Like all measurements, the pressure data obtained from the engine test cell needs to verified for some of the common errors before they can be used further for the burn rate analysis and calibration. The test cell data was analysed using a software known as AVL Concerto.

AVL Concerto is a graphical data evaluation and visualization software package designed to handle different kinds of data acquired on an engine or vehicle test bed. It is an ideal tool for professional data browsing and data management as well as for presentation, calculation, report generation and batch processing of the acquired data. It contains pre-built macros for performing standard calculations such as heat release analysis, zero line pressure correction, filtering, etc. The tool also gives flexibility to the user to write their own macros to process and visualize the data (AVL, 2015). This tool was extensively used during the preliminary data analysis process where custom scripts were written to validate the input data from the test cell.

There are three common errors, which can be found in the pressure data acquired from the test cell. The description and methods to identify these errors are explained below.

2.3.1 ENCODER ERROR

Encoder error pertains to the error in the relative phasing between the signals from the pressure transducer and the crank angle encoder. It is important to determine the phasing of a measured cylinder pressure trace with high accuracy (Davis et al., 2006). Incorrect phasing (encoder error) will lead to error in the heat release curve, both in shape and size and hence an incorrect thermodynamic information about the performance characteristics of the engine (Davis et al., 2006). An error of 1 degree in CA results in an error of 10% in the heat release, and 5% to 25 % in the instantaneous pressure (Mark Bos, 2007).

There are two ways to determine the encoder error. (Davis et al., 2006).

1. TDC sensor.
2. Motored engine pressure trace.

1. **TDC sensor**
   A TDC sensor mounted on the injector or spark plug produces a voltage signal as a function of piston movement and hence helps in the correct TDC determination. This is the recommended method since it is not affected by errors in pressure values caused due to incorrect pegging, intra-cycle drift, etc. (Davis et al., 2006).

2. **Motored engine pressure trace**
   In an ideal motored engine representing a closed adiabatic thermodynamic system, the energy exchange during compression and expansion stroke will balance out completely, i.e. the work done during compression will be completely recovered during the expansion stroke resulting in the peak pressure centered at compression TDC. However real engines have losses in the form of heat transfer, crevice effects and blow-by. This causes the point of maximum pressure to shift within 1 degree before the compression TDC. (Davis et al., 2006) & (Wang, 2014).

2.3.2 PEGGING ERROR

Piezo electric transducers are the most commonly used sensors for measuring the pressure trace inside the cylinder. They work by generating a charge relative to a change in pressure. This charge is converted to corresponding voltage using a digital circuit. It is therefore important to peg the pressure against a known reference at every cycle. This creates an on-the-fly transfer function which is used through the remainder of the cycle. (Maurya et al., 2013).

The general representation of the transfer function is shown in Eq. 2.18.

$$P(\theta) = P_{peg} + Gain\ (V(\theta) - V(\theta_{peg})) \qquad (2.18)$$

Where, P_{peg} is the pegged pressure , $Gain$ is the sensor gain value in bar/volt which is fixed for a given sensor, $V(\theta)$ is the voltage in Volts at a given crank angle θ and $V(\theta_{peg})$ is the voltage at the crank angle where the pressure is being pegged.

Parameters affected by incorrect pressure pegging are, Instantaneous Heat Release, Cumulative Heat Release, crank angle of peak pressure, burned mass fraction, bulk charge temperature, polytropic coefficient. (Maurya et al., 2013).

There are two ways to check for pegging error.

1. Polytropic coefficient
2. Pressure shift

1. **Polytropic coefficient**
   The polytropic exponent is related to the specific heat of the gases and the rate of heat transfer across the cylinder walls. It has been found that for a DI Diesel engine, the polytropic coefficient during the initial part of the compression process (-90 to - 40 degrees BFTDC) is in the range of 1.35 to 1.37 (Günter et al., 2002). So, the pegged pressure must have a polytropic index within this window. Increase in dilution also affects the polytropic index of the gases.

2. **Pressure shift**
   It is known that for an untuned intake system, the intake pressure in the inlet manifold matches the cylinder pressure at inlet BDC. The maximum error between the reference (intake) and cylinder pressure should be 200 milli bar (Wang, 2014).

2.3.3. ERROR DUE TO THERMAL SHOCK

During the combustion stroke, a large amount of heat energy is released. The high heat flux can cause the offset value of the piezo electric sensor to change momentarily. This is known as thermal shock. Generally the sensors have very low time constants and recover before the start of next pegging cycle. However, in cases where the sensor doesn't recover, intra cycle drift in the pressure may occur. This would lead to inaccuracies in the pressure readings (Davis et al., 2006).

Thermal shock can be detected by analysing the Average Exhaust Absolute Pressure (AEAP) between 240 to 320 degrees after firing TDC. For good quality measurements the standard deviation of AEAP must be within 4kPa (Davis et al., 2006).

2.4 ENGINE BURN RATE ANALYSIS

In order to calibrate the predictive combustion model, engine burn rate data is required from tests. Unfortunately, it is difficult to measure the burn rate during measurements, thus the the cylinder pressure is measured instead.

In GT-Power by knowing the cylinder pressure, the burn rate can be calculated and vice versa. It uses a 'reverse run' simulation to estimate the burn rate from the cylinder pressure and a 'forward run' simulation where the cylinder pressure is estimated based on the burn rate (GT-Suite, 2013). For calibration of the combustion model the reverse run simulation is always used.

For fuel burn rate calculations GT-Power divides the cylinder into two zones (GT-Suite, 2013). First zone, the unburnt zone consists of unburnt air-fuel mixture, the fuel that is being injected in the zone at that instant and the residuals at IVC. Second zone, the burnt zone is populated in subsequent time steps by burning the mixture from the unburnt zone. The amount of mixture being transferred from unburnt zone to the burnt zone is defined as the burn rate (GT-Suite, 2013).

2.4.1 TYPES OF BURN RATE ANALYSIS

Within GT-Power there are two ways of estimating the burn rate using reverse run simulations, namely Three Pressure Analysis (TPA) and Cylinder Pressure Only Analysis (CPOA) (GT-Suite, 2013). Both these methods require an input of the measured cylinder pressure resolved as a function of crank angle. These two methods are described below in detail.

➢ Three Pressure Analysis (TPA)

TPA derives the burn rate for an operating condition based on three measured pressures namely intake, exhaust and cylinder pressure (GT-Suite, 2013), (Wang, 2014). It is typically a reverse run calculation, wherein the amount of fuel transferred from the unburned to the burned zone is iterated in each time step until the simulated pressure matches the measured cylinder pressure.

The initial values of volumetric efficiency, trapping ratio and residuals quantities are predicted based on the measured port pressure and average temperature imposed in the end environment (GT-Suite, 2013), (Wang, 2014).

There are two variations of TPA analysis, namely 'TPA steady' and 'TPA multicycle' (GT-Suite, 2013). The former uses measurement data resolved against crank angle over a single cycle while the later requires measurement data over multiple cycles. The advantage of 'TPA multicycle' is that it can better account for cyclic variations.

- **Cylinder Pressure Only Analysis (CPOA)**

CPOA estimates the burn rate for an operating condition based on the measured cylinder pressure only.

The burn rate calculations in CPOA is quite similar to the TPA but, the major difference between the two is that in CPOA the initial values of volumetric efficiency, trapping ratio and residuals quantities cannot be estimated and must be provided as an input (Wang, 2014).

The main limitation of this approach is the difficulty in estimating the trapping ratio and the residuals in the test cell (GT-Suite, 2013), (Wang, 2014).

3 METHODOLOGY

The methodology followed for calibration of the DI pulse model is shown in figure 3.1. The first step (section 3.1) includes data collection from the single cylinder test rig. In this step, a set of 28 points were chosen based on the RDE cycle at Volvo cars for operating the engine and collecting the data. The data collection included dynamic intake, exhaust and in cylinder pressure along with injection strategy, residuals, swirl and emissions (CO, HC and NO_x).

The next step (section 3.2) included, performing initial quality check of the data in AVL Concerto. The primary objective of this step was to verify the input data for three errors, namely encoder, pegging and thermal shock error. The secondary objective was to check for erroneous heat release data.

The following step was to obtain an injection profile in GT-Power. For this thesis, a GT-Suite injector model was obtained from the supplier. As already explained in section 2.2.3.2, the accuracy of the injection profile is strongly linked to the calibration quality of the model. Henceforth, the simulated injection profile obtained from the GT-Suite injector model was validated against the data obtained from flow bench at Volvo cars.

Once the above steps were completed, TPA analysis (section 3.4) was performed on the input data. The primary input for TPA is injection profile and the three pressures - input, exhaust and in cylinder pressure along with other operating data obtained from the test cell. The measured cylinder pressure is validated by performing a series of detailed automated consistency check on the input data. The other important output from the TPA is the trapped quantities which is difficult to measure physically in the test cell.

The next step was to perform CPOA (section 3.5) analysis. This is to validate the results obtained from TPA analysis. The inputs to the CPOA model are the trapped quantities obtained from the TPA and the measured pressure. If the trapped quantity predictions out of TPA are good, then the simulated pressure obtained from CPOA should match the one obtained from TPA analysis.

Once all the data validation was completed, the calibration of the model was carried out by selecting 25 points. A DOE of the combustion model multipliers was run for the 25 cases. The final set of multipliers were selected from an optimization tool supplied by the Gamma Technologies. Once the calibration process was completed, the multipliers obtained were used to validate the model against 3 points. The steps involved in the calibration process have been explained in detail below.

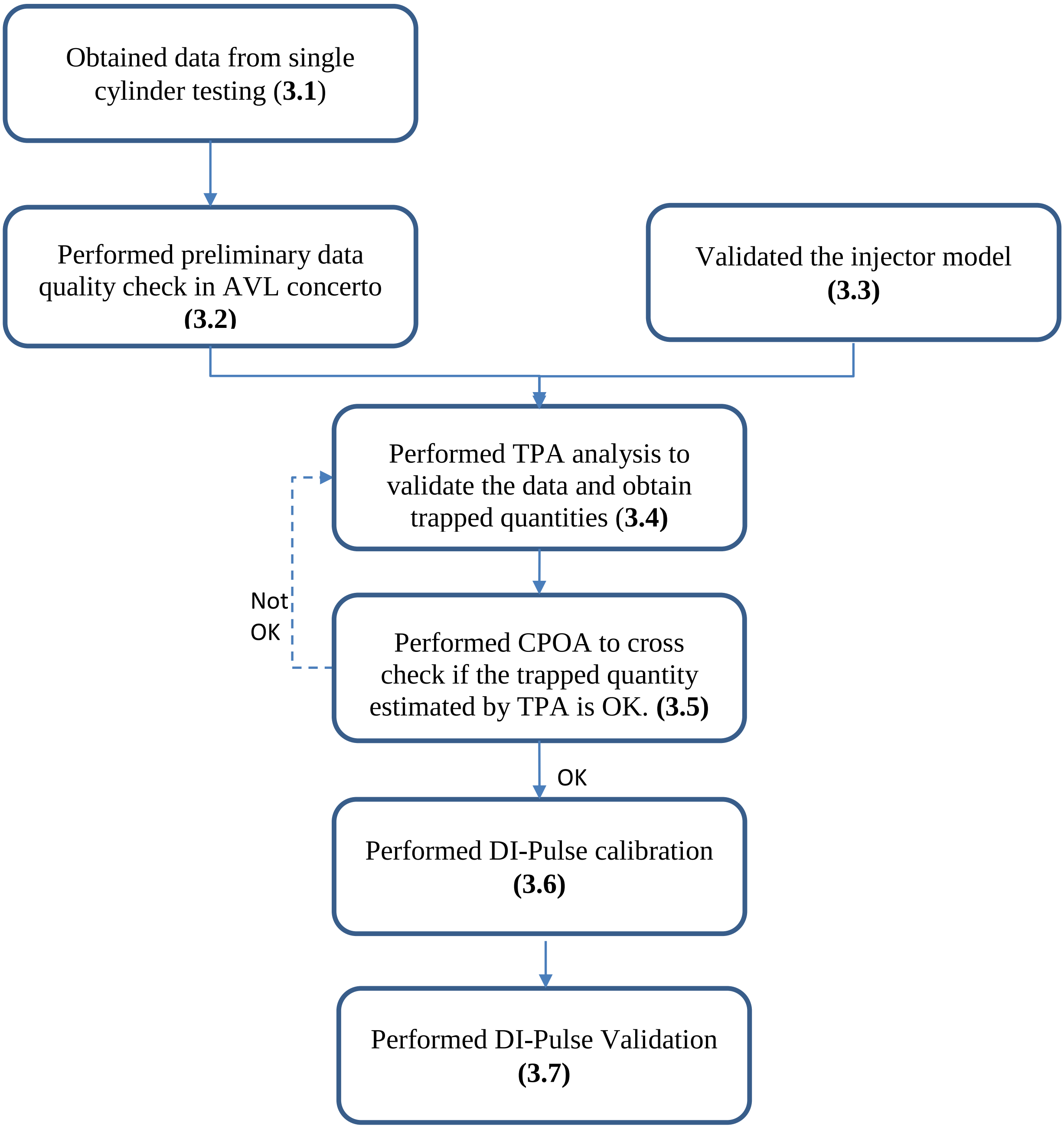

Figure 3.1: Process followed for the calibration of DI Pulse model

3.1. SINGLE CYLINDER TEST

For any calibration process, test data is the key. For this thesis, data such as pressure trace at the intake manifold, exhaust manifold and cylinder, the emissions at EVO including HC, CO & NOx, and residuals at IVC were measured in a single cylinder test rig at Volvo Cars.

In order to get a representative combustion model, Gamma Technologies recommend the calibration to be performed for at least 25 operating points with a good spread on the engine map.

Figure 3.2 shows the 28 operating points that were used to perform the tests. Out of the 28 points, 25 were used for calibration and 3 were used to evaluate the predictive capability of the model. These points were picked from the Real Drive Emission (RDE) cycle used at Volvo Cars as it will be used for future emission certification in Europe replacing the currently used NEDC driving cycle. Since one of the major expectations of the predictive combustion model is to be able to predict the combustion characteristics of various operating points with differing level of EGR and injection strategy, this was an important criteria in choosing the points. The variation of EGR level among the different points chosen is shown in figure 3.3. The variation in number of injections is shown in Table 3.1. The chosen points also include key operating characteristics such as maximum torque and maximum power.

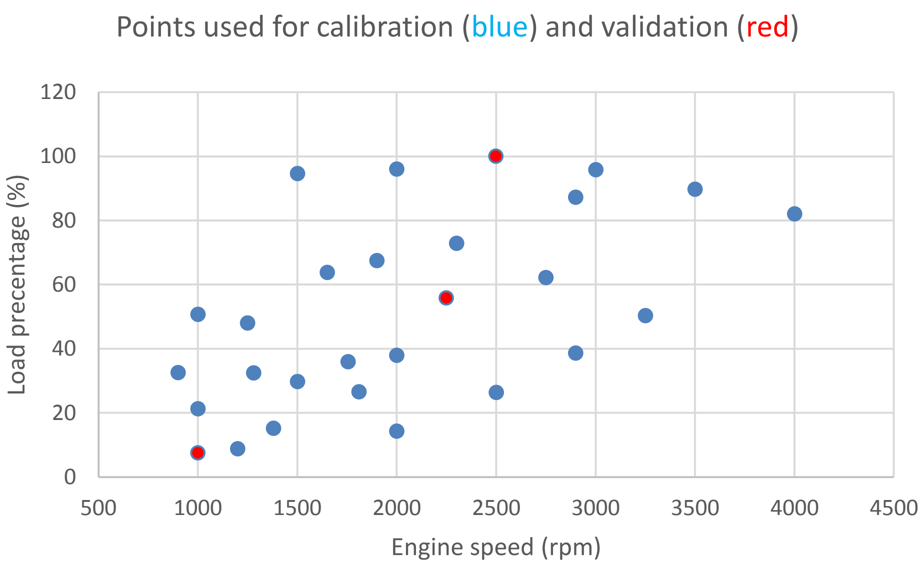

Figure 3.2 – Points used for calibration (blue) and validation (red)

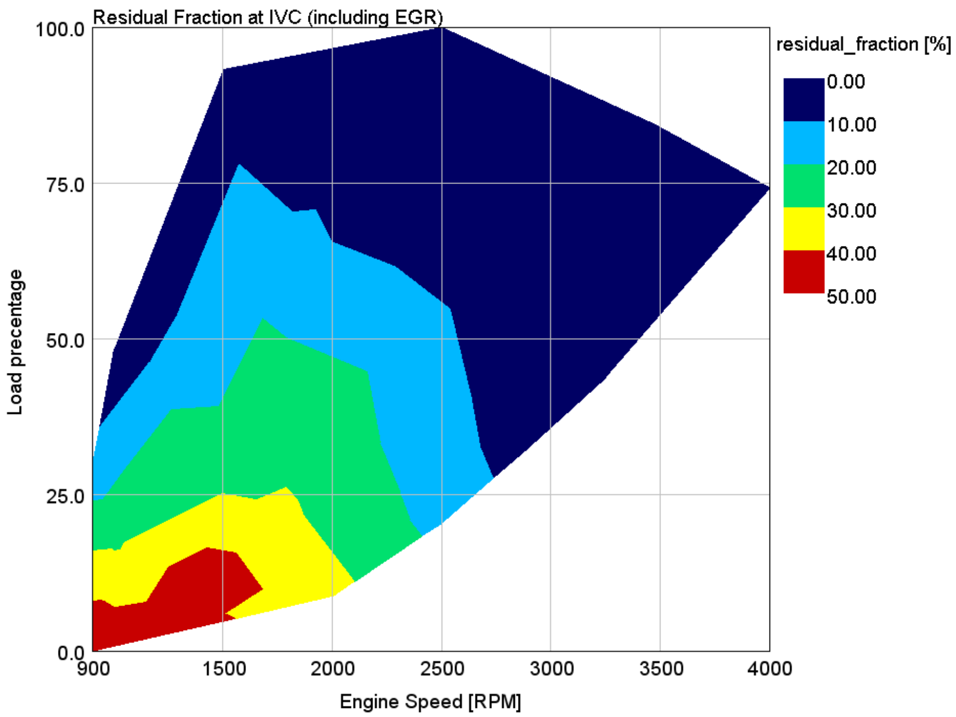

Figure 3.3: Plot of EGR against load and speed

Table 3.1: Variation in number of injection

Number of Injections	Number of Points
2	2
3	15
4	11

3.1.1 TEST PROCEDURE

This section includes a brief discussion about the test procedure followed. Prior to starting the test, a Rig Stability Check (RSC) was performed. During RSC the engine was run at 2000 rpm and a series of automated checks were performed to identify potential deviation in the measuring equipment. A fixed speed of 2000rpm is chosen to have a fixed baseline value. Once the RSC checks were successfully completed, the engine was run at the desired operating points as shown in figure 3.2. The test procedure is enumerated below.

1. The heat release curve for the chosen operating point was loaded in AVL Concerto.
2. The engine was motored to the desired speed.
3. The operating variables such as swirl flap position, EGR percentage, intake pressure, exhaust backpressure and base injection strategy were initialized.
4. Once the operating variables stabilized, the obtained heat release curve was compared against the baseline.
5. The injection quantity and pulse separation was modified to minimize the deviation in the heat release curve.
6. Once the curves matched, the desired IMEP and lambda values were used to validate the point against the base data.
7. After validation, 100 engine cycles were recorded for each operating point.

3.2 TEST DATA VERIFICATION

Once the tests were performed in the single cylinder test cell, the quality of data had to be validated. Measurement data is seldom perfect and an erroneous dataset can impact the quality of TPA analysis and further the quality of the calibrated model. The most common errors in the measured data are encoder error, pegging error and error due to thermal shock. The description of these error have explained in section 2.3. The errors were verified using AVL Concerto.

3.2.1 ENCODER ERROR

As explained in 2.3.1 there are two ways to check for encoder error. Either using a TDC sensor or by analysing the motored pressure trace. Since the test rig at Volvo Cars does not have a TDC sensor, the motored pressure trace was analysed and the peak pressure was ensured to occur within .6 to 1 deg. before compression TDC as shown in figure 3.4. The motored pressure trace was obtained at 2000 rpm. The speed of 2000 rpm was based on Rig Stability Check (RSC) as discussed in section 3.1.1

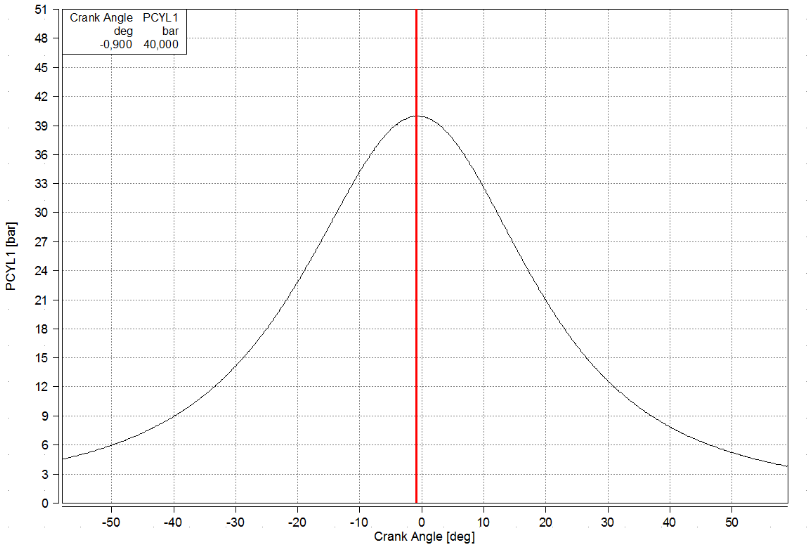

Figure 3.4 – Motored pressure trace for encoder error verification

3.2.2 PEGGING ERROR

As explained in 2.3.2 there are two ways to verify the pegging error. Either using the polytropic coefficient or by estimating the cylinder pressure shift. Both these methods were used in this thesis. Firstly the polytropic coefficient was verified to be within 1.35-1.37 during the compression stroke between -90 to -35 CAD before compression TDC. Secondly the pressure difference between the cylinder pressure trace at intake BDC and average intake manifold pressure between ± 5 CAD of intake BDC was verified to be within 200 milli bar. Fig 3.5 shows one of the case where the deviation was maximum but still found to be within the recommended limit.

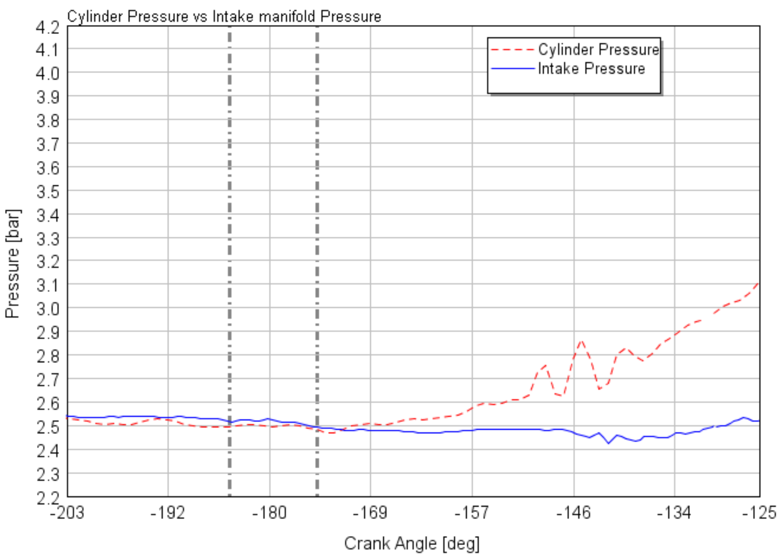

Figure 3.5 – Plot of cylinder pressure vs intake manifold pressure to verify pegging error

3.2.3 THERMAL SHOCK

As explained in 2.3.3 the presence of thermal shock can be detected by analysing the Average Exhaust Absolute Pressure (AEAP).

The AEAP was calculated in the window between 240 to 320 CAD after firing TDC and the standard deviation was calculated and verified to be within 4kPa as shown in fig 3.6.

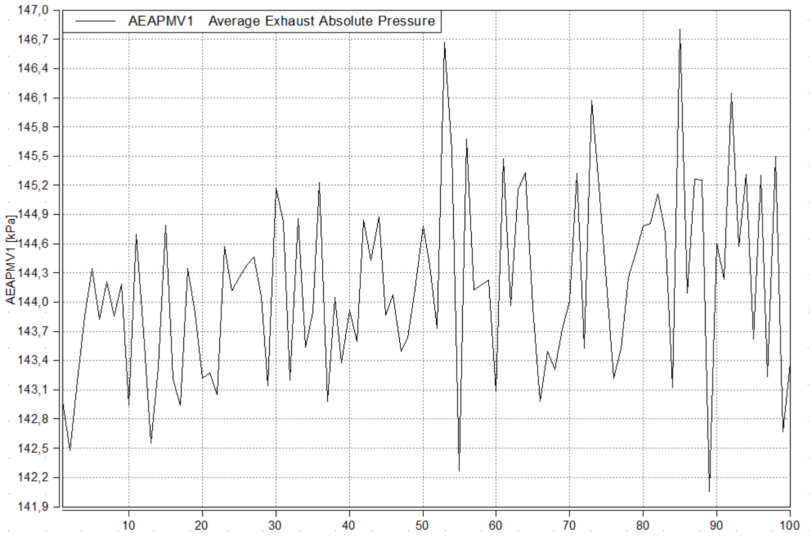

Figure 3.6 – Average exhaust absolute pressure for 100 cycle

3.3 INJECTOR RATE PROFILE

The accuracy of the DI-Pulse model depends significantly on the accuracy of the injection rate profile. Hence it is important to obtain an accurate injection profile.

The injection rate profile for the DI-Pulse can be specified in three ways.

- Predictive injector model.
- Injection rate map.
- Data from Injector flow rig.

Each of the above mentioned methods have their own benefits and drawback as explained below.

➢ Predictive injector model

A GT-Suite predictive injector model as shown in fig 3.7 is the recommended method by Gamma Technologies due to their ability to handle valve dynamics and hydro mechanical interaction on a variety of operating points. The typical input for an injector model is the electrical signal from the actuator and the output is the rate profile and mass injected per pulse. However, the major drawbacks to this method is that simulation times can be significantly high when integrated to the engine model, accurate modelling of the all the components is difficult and validation against test data is required to ensure the accuracy of the model.

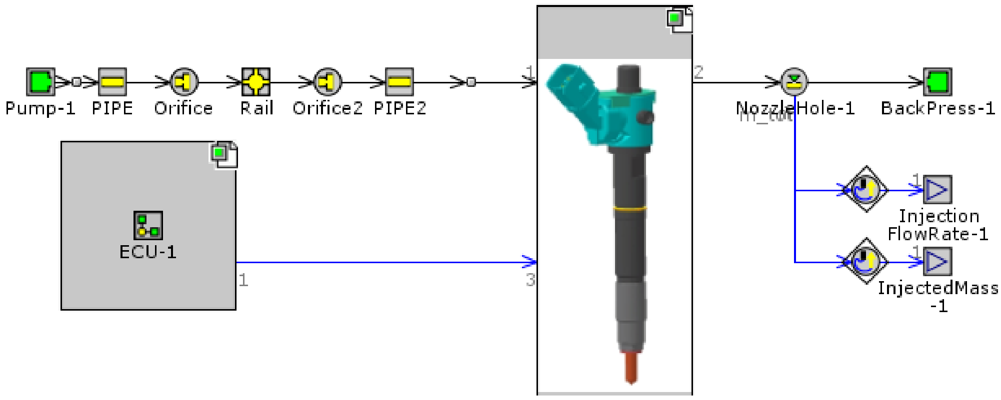

Figure 3.7: GT-Suite Model of a predictive injector (Denso, 2015)

➢ Injector Rate Map (IRM)

The Injector Rate Map (IRM) consists of the injection rate profile for a given rail pressure and energizing time as shown in Fig 3.8. This map can be populated either from the predictive injector model or with data from the injector flow rig test. The typical input for an IRM is the start timing of each pulse and injected mass per pulse. The output is the rate profile. The main benefits of the IRM are its fast run time and scalability. However it cannot account for the instantaneous variation of rail pressure and pulse to pulse interactions.

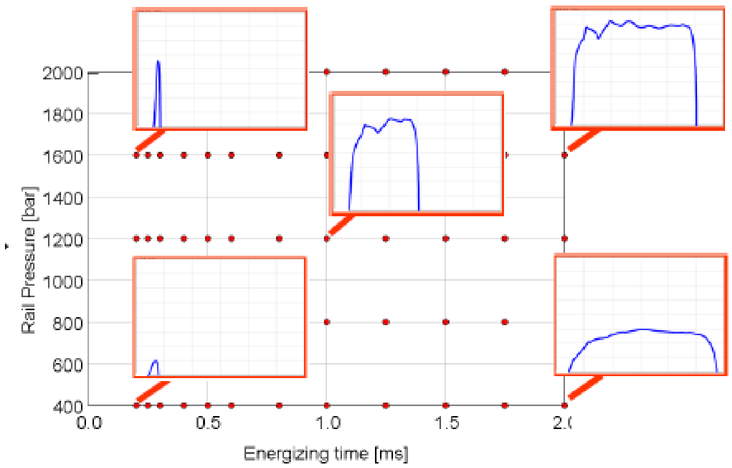

Figure 3.8: Injector Rate Map used in GT-Power(Wang, 2014)

➢ Injector Flow Rig

The rate profiles obtained from the injector flow rig may either be used to populate the IRM or directly used for the combustion model calibration. Although this method avoids the inaccuracies caused by modelling, the process may be time consuming, there may be errors in measurements and there may be noise in the data obtained which needs to be filtered. The model scalability is also a problem since tests have to be conducted each time a new point is to be included.

For this thesis initially it was intended to use the predictive injector model obtained from the injector manufacturer. However on validating the model with data from the injector flow rig for 5 points whose operating characteristics is shown in table 3.2, it was found that the model was significantly inaccurate both in terms of timing and quantity delivered. To overcome this problem the injection pressure was scaled up. Although this helps reduce the error in quantity of fuel, it does not improve the error in injection timing. Hence the predictive injector model could not be used.

The next best alternative would have been to obtain the injection data for all the 28 points from the flow rig and use them further for all the analysis. However the flow rig at Volvo Cars was not available at that moment.

Hence the final alternative was to generate an Injector Rate Map (IRM) populated from the predictive injector model. The inputs to the IRM were the scaled up rail pressure, start of injection of each pulse and mass of fuel required for each pulse. The mass per pulse was obtained using the predictive injector model with the scaled up rail pressure. The start of injection for each pulse was obtained by adding a constant hydraulic delay of 200 μs to the start of electrical trigger of each pulse. The IRM worked relatively well when compared with the flow rig data for the same 5 points mentioned in table 3.2.

Table 3.2: Injection Strategy for validation points

Point	Rail Pressure (bar)	No. of pulses
1	801.7	5
2	790.5	4
3	820.2	4
4	940.4	5
5	730.4	5

3.4 THREE PRESSURE ANALYSIS (TPA)

As explained in section 2.4, the TPA is used to derive the burn rate based on the input measured pressure trace. Apart from this there are two primary reasons for performing the TPA analysis. Firstly it helps in calculating the trapped quantities at Intake Valve Closing which is required for the calibration. This is essential because it is extremely difficult to measure these trapped quantities in the test cell and TPA helps predict them. The second reason for performing the TPA is that they help to validate the quality of the measured pressure trace before it is used for the calibration.

The primary inputs for the TPA are the three pressures - intake, exhaust and in-cylinder pressure trace. Other secondary inputs include injection profile, emissions, measured air mass and fuel injection profile.

As a part of analysis, GT-Power performs several consistency checks on the input data to access its overall quality. The associated metrics are described below.

- **BMEP**: The BMEP for a cycle is equal to the algebraic difference between IMEP and FMEP. If the above relation is not satisfied, then it could indicate a problem with estimated IMEP and hence the input pressure data. It should be noted that the FMEP data should be reliable to avoid wrong results.
- **Pressure Smoothing**: The measured pressure profile should be reasonably smooth. As a part of the pressure analysis, GT-Power uses a low pass filter (5 kHz) on the input data. After smoothing, an RMS value is calculated between the smoothed and raw pressure curve. If the RMS is greater than .02 bar then an error is flagged, as over-smoothing can cause a loss of data.
- **Cumulative Burn Rate**: In a DI diesel engine, the combustion happens only after the fuel has been injected into the cylinder. So in theory no fuel should burn before the start of injection. This is verified by calculating the integrated burn rate upto the designated start of analysis (SOI), which should be close to zero.
- **Changes in fuel LHV**: The fuel Latent Heat Value (LHV) multiplier is an indicator of the error in the cumulative burn rate. It indicates the change required in the LHV of the fuel to complete the analysis. Ideally it should be close to 1 with a maximum deviation of +/-5%. An error could indicate a problem with the model inputs.
- **Combustion efficiency target**: It indicates the change in the LHV required to achieve the target combustion efficiency or the burnt fuel fraction specified. If the required LHV change is more than 5% then it indicates an error with the pressure analysis.
- **Apparent indicated efficiency**: If the calculated efficiency is unrealistic (>45%) it may indicate an error with the input data.
- **Air and fuel mass**: This consistency check is performed to ensure that the measured and the simulated air and fuel flow rate are within +/- 5% of the measured value. An out of bound value may indicate possible error with gas exchange or fuel mass delivery.
- **Fuel ratio error:** In TPA analysis, the simulated air fuel ratio is compared to the measured value obtained from the test cell data. If the deviation is more than +/- 5%, an error is flagged.

If the above mentioned criteria are not satisfied, GT-Power indicates an error code specific to each error. These could indicate inaccuracies in either the measured data or incorrect inputs to the model.

The TPA analysis was performed for all the operating points. The consistency checks and pressure match between measured and simulated was verified for all points. Any errors encountered in TPA was rectified.

Despite well measured data from the test cell, in some cases the consistency checks was not satisfied or the simulated pressure trace did not match well with the measured pressure trace due to wrong inputs to the model. These were primarily incorrect compression ratio and valve timing. The causes of these errors and how they were rectified are explained below.

3.4.1 COMPRESSION RATIO ADJUSTMENT

The geometric compression ratio of an engine remains constant however, the dynamic compression ratio of an engine varies as a function of load and speed. It is extremely difficult to measure the compression ratio for each operating point in the test cell, hence the TPA was used to estimate it. This was done by iterating the compression ratio to get a good match of the simulated and measured pressure trace until the designated start of injection. figure 3.9 and figure 3.10 show an example of one of the cases that required maximum adjustment to the compression ratio, which was from 15.8 to 14.8. However the final calibration model is represented by an average of all the dynamic compression ratio to facilitate model scalability.

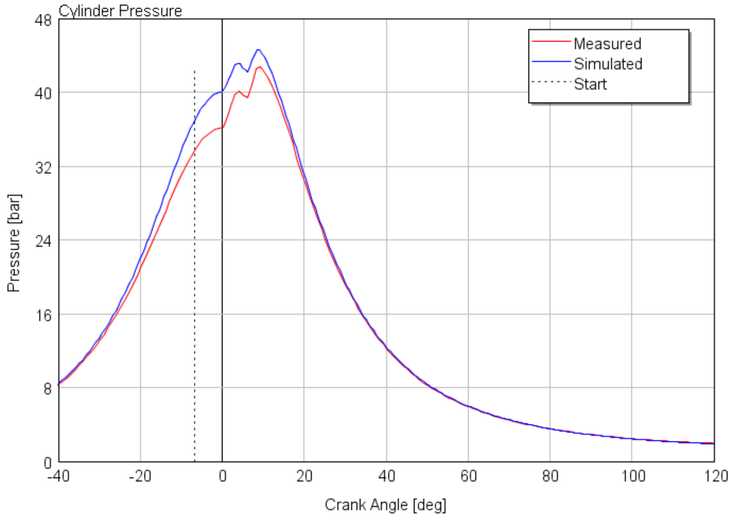

Figure 3.9: Measure vs Simulated Pressure trace with geometric compression ratio of 15.8

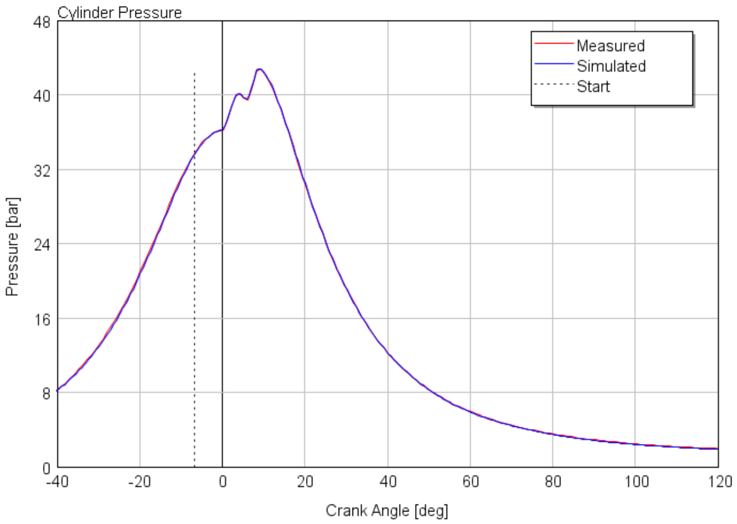

Figure 3.10: Measure vs Simulated Pressure trace with dynamic compression ratio of 14.8

3.4.2 VALVE TIMING ADJUSTMENT

The TPA model used in GT-Power has a fixed valve timing without any valve dynamics being modelled. However, in a real engine the valve timing varies slightly as a function of speed and load due several factors such as valve lash, inertia, thermal effects, etc. These lead to discrepancy in the valve timing between the real engine and the TPA model. An incorrect valve timing leads to variation in the estimated trapped quantities and deviation between the simulated and measured airflow rate. This error was corrected by varying the valve timing until the simulated and measured air flow rates matched.

3.5 CYLINDER ONLY PRESSURE ANALYSIS (CPOA)

The TPA analysis was performed to derive the burn rate and the trapped quantities from the test cell data. However, to ascertain the accuracy of the trapped quantities estimated by TPA, the CPOA was performed. The main difference between TPA and CPOA is that, unlike TPA the CPOA is not a complete engine model. It includes only the injector, cylinder and crank train as shown in figure 3.11. Hence the simulated cylinder pressure trace at IVC in CPOA is calculated based upon the trapped quantities obtained from TPA. Therefore if the estimation of trapped quantities in TPA is correct then the simulated pressure trace out of CPOA and TPA would match.

Henceforth the CPOA was performed for all the 28 points undertaken for the TPA. An example of the measured vs simulated pressure trace in TPA and CPOA analysis for a specific point is shown in figure 3.12 and figure 3.13.

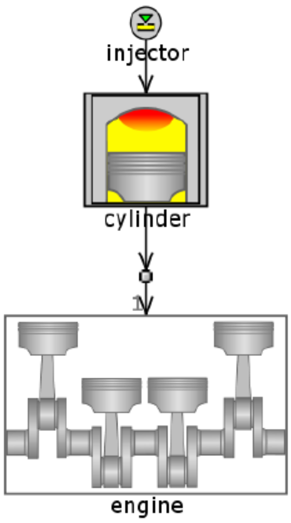

Figure 3.11: CPOA model in GT-Power

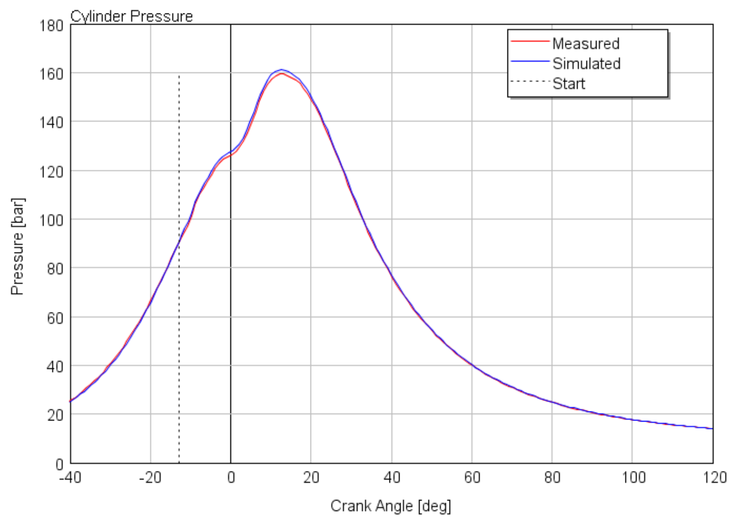

Figure 3.11 – Measured vs Simulated Pressure trace in TPA analysis

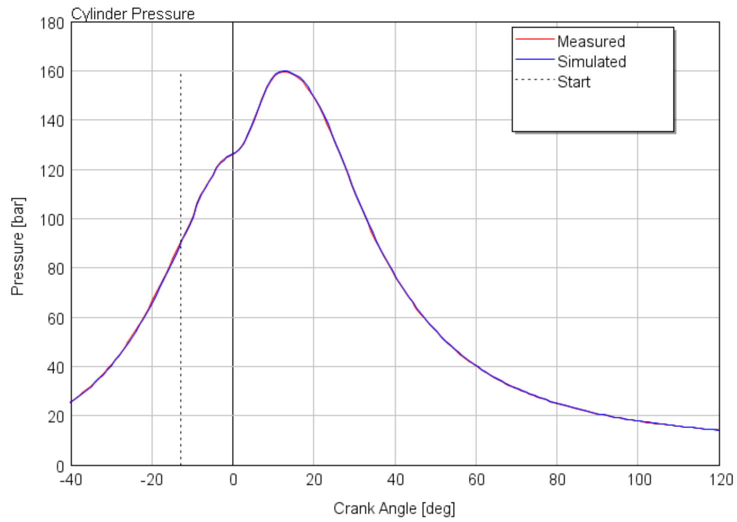

Figure 3.12 – Measured vs Simulated Pressure trace in CPOA analysis

3.6. DI PULSE CALIBRATION

The next step in the model calibration process is to obtain a set of four multipliers for the combustion model namely entrainment rate, ignition delay, premix combustion rate and diffusion combustion rate multipliers. Detailed description of these multipliers have been explained in section 2.2.3.2.

Out of the 28 points where the test data was obtained, 25 points were used for calibration. The remaining 3 points were used to evaluate the ability of the DI-Pulse model to predict the combustion characteristics.

The model for the DI-Pulse calibration is similar to the CPOA model. The cylinder, crank train and injector were isolated and a Design of Experiments (DOE) of the four multipliers was run for all the operating points, which were found to be satisfactory in the TPA and CPOA. Once the DOE was complete, the optimal constants were chosen in such a way as to minimize the burn rate error in all the cases. These optimal constants were then used to rerun the model without the DOE and the results were analysed.

The quality of the calibration was analysed by observing the measured vs. predicted burn rate plots. They should match closely for all the operating points. Additionally Gamma Technology recommended to observe the average RLT (result) errors of the parameters shown in table 3.3. These values were obtained by Gamma Technologies from the results provided by a number of OEMs who have performed the same model calibration on a variety of engines varying from 0.4L to 5L per cylinder.

Table 3.3: Suggested error threshold for DI Pulse calibration parameters

Parameter	Average Error
Burn rate (%)	.0054
IMEP (%)	2.2
CA50 (deg)	0.9
Max. Pressure (bar)	2.8
NOx (ppm)(%)	20

Once the optimal constants were chosen from the results of the DOE, minor manual fine-tuning was done in order to improve the results. For fine tuning the multipliers their influence on the burn rate and cylinder pressure trace was first understood.

- **Entrainment rate multiplier**

  This multiplier influences the rate at which the fuel injected entrains the air and residual gases in the cylinder. A higher value leads to a larger amount of fuel entrained in a shorter period of time. Hence as can be seen in figure 3.14 and figure 3.15 the premix peak and the diffusion peak increase significantly due to faster rate of combustion. The crank angle for 50% burn also reduces as shown in figure 3.16.

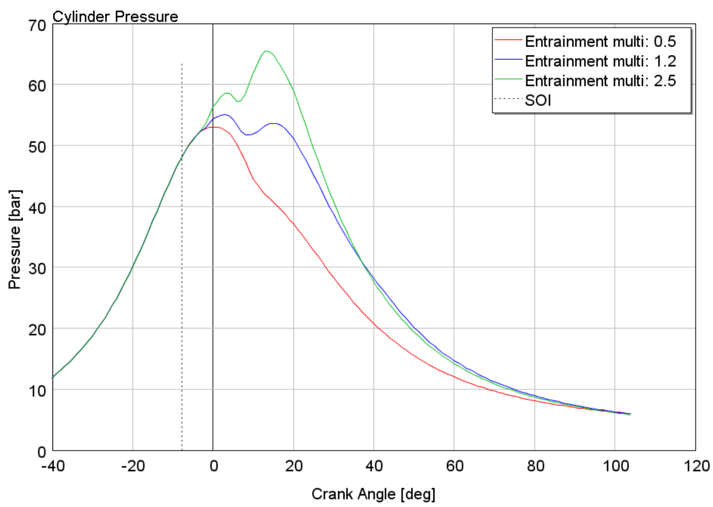

Figure 3.14: Pressure trace for different Entrainment rate multipliers

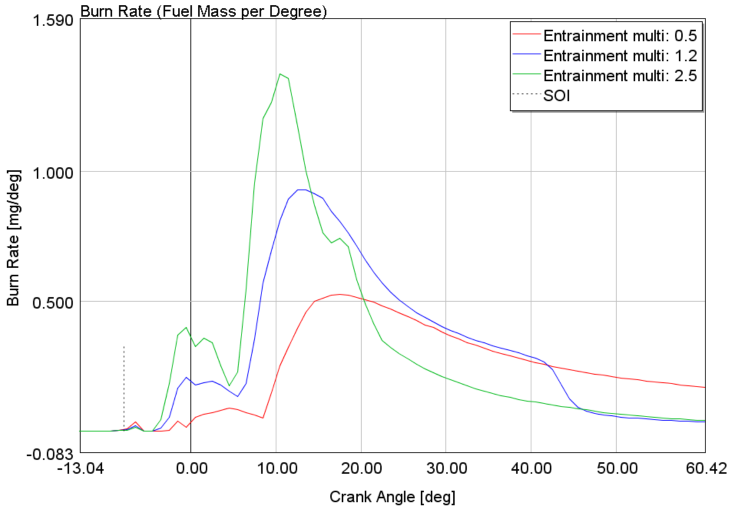

Figure 3.15: Burn rate for different Entrainment rate multipliers

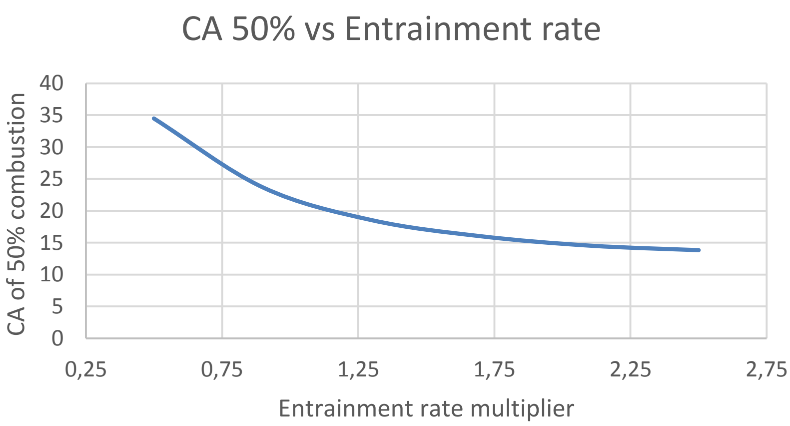

Figure 3.16: CA 50% burn vs Entrainment rate multiplier

- **Ignition delay multiplier**

  The ignition delay multiplier influences the time taken between fuel injection and start of combustion. A higher value increases the delay and hence more fuel would be accumulated before the start of premix combustion. This increases the peak during the premix phase as shown in figure 3.17 and 3.18. It also retards the start of combustion as shown in figure 3.19.

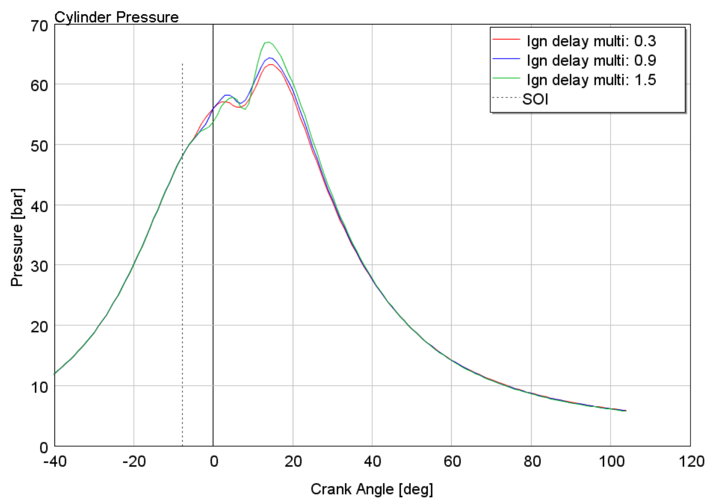

Figure 3.17: Pressure trace for different Ignition delay multipliers

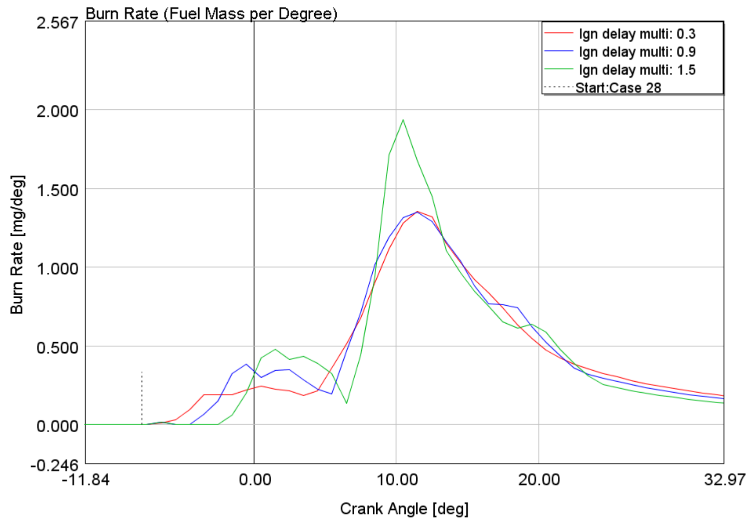

Figure 3.18: Burn rate for different ignition delay multipliers

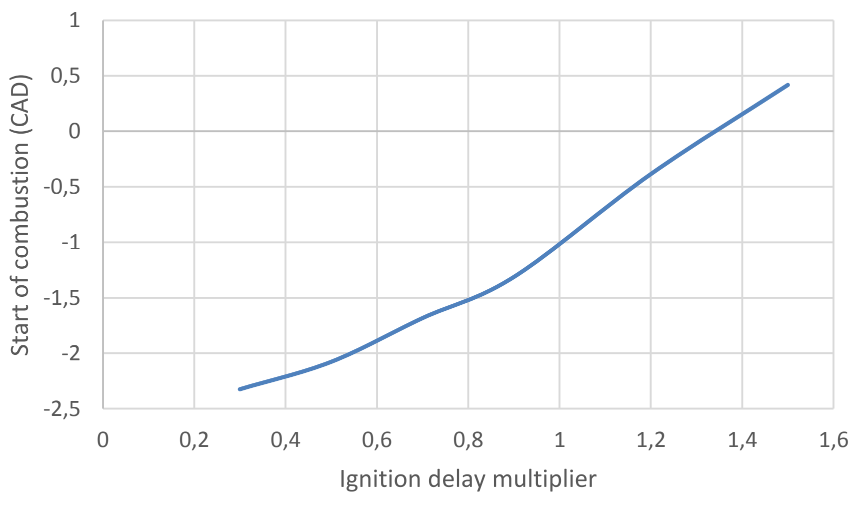

Figure 3.19: Start of combustion vs ignition delay multiplier

- **Premix combustion rate multiplier**

  This multiplier has an influence primarily on the rate at which the premix combustion takes place. As shown in figure 3.20 and figure 3.21, a larger value increases the slope of the premix curve. It has a very small effect on the premix peak and the diffusion peak.

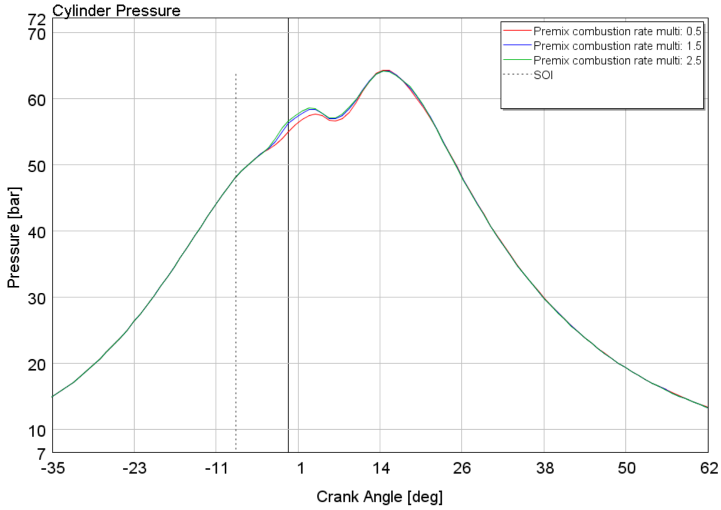

Figure 3.20: Pressure trace for different Premix combustion rate multipliers

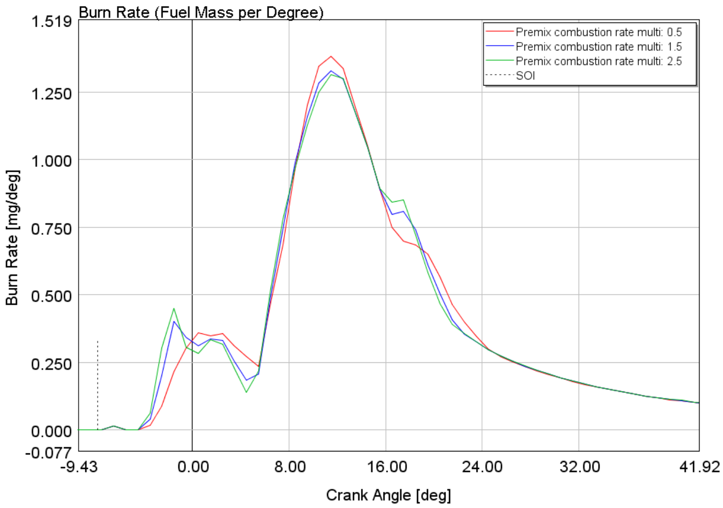

Figure 3.21: Burn rate for different Premix combustion rate multipliers

- **Diffusion combustion rate multiplier.**

  This multiplier primarily has an influence on the rate of diffusion combustion and the diffusion peak. A larger value increases the slope of the diffusion curve and the diffusion peak. It has a very small effect on the premix combustion as shown in figure 3.22 and figure 3.23. The magnitude of increase in maximum pressure is shown in figure 3.24.

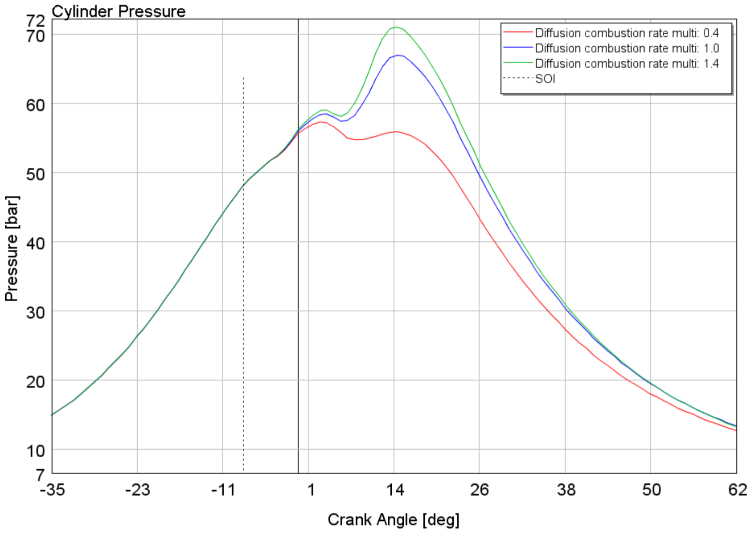

Figure 3.22: Pressure trace for different Diffusion combustion rate multipliers

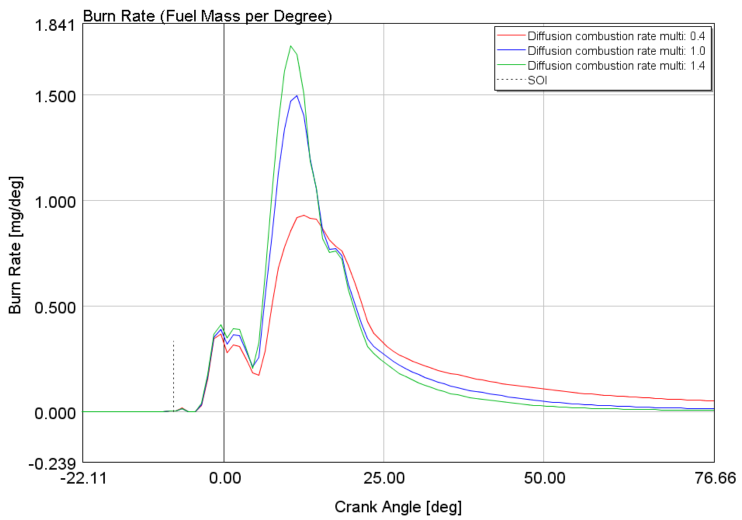

Figure 3.23: Burn rate for different Diffusion combustion rate multipliers

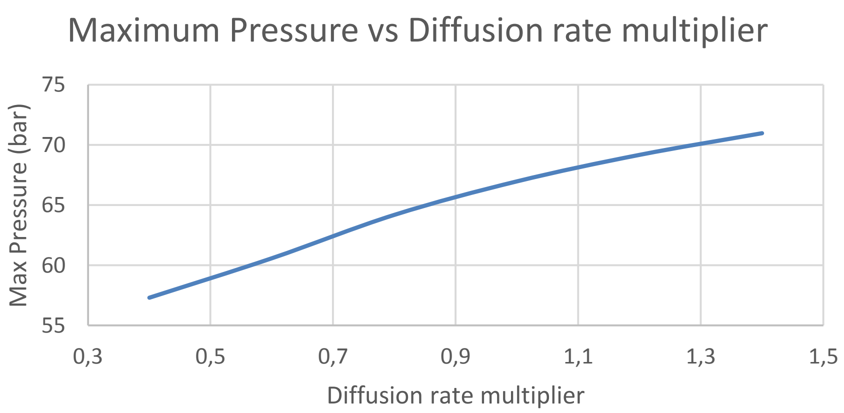

Figure 3.24: Max. Pressure vs Diffusion rate multiplier

3.6.1 NO_X CALIBRATION

The emission model in GT-Power predicts only NO as opposed to real engine out NOx which consists of NO and NO2 molecules. This is primarily because GT-Power uses Zeldovich mechanism, which models only NO emissions. Hence the predicted NO from the model was calibrated against the measured NOx data. This was done with an assumption that some of the NO molecules predicted by the Zeldovich mechanism would be oxidized to NO_2. Thus predicting the total particle count of NO would be the same as predicting the total NO_X.

3.7 DI-PULSE PREDICTION

The final step in the thesis is to evaluate the ability of the calibrated DI-Pulse model to predict the combustion characteristics. The ideal way to evaluate the prediction quality is by performing a sensitivity analysis. It includes running sweeps of EGR, injection timing, and swirl flap position in low, medium and high load region against different engine speeds. However, due to unavailability of such test data, the comparison had to be made using only 3 points amongst the 28 points for which test data had been collected. Since the rest were used for model calibration. The first point was at low speed and low load with high EGR and Swirl. The second point was at mid speed and mid load with moderate level of EGR. The third point was the maximum torque point with no EGR and swirl. The operating points are tabulated as shown in table 3.4

Table 3.4: Operating point selection for DI Pulse prediction

Point	Speed (rpm)	Load %	EGR (%)	Swirl (%)
4	1200	9.27	39.99	18.41
26	2250	56.66	13.43	0
18	2500	100	0	0

4 RESULTS AND DISCUSSION

In this section the results and discussions from the fuel injector validation, three pressure analysis, cylinder pressure only analysis and finally the quality of calibration and validation of the DI-Pulse model have been presented.

4.1 INJECTOR MODEL VALIDATION

As explained in section 3.3, the recommended method for specifying the fuel injection profile is using a predictive injector model. This injector model was obtained from the injector manufacturer. Unfortunately the accuracy of the injection profile was found to be poor, when compared against the injector flow rig data obtained at Volvo Cars for five injection strategies. Figure 4.1 shows the comparison between the GT-Suite injector model and the pump rig data for one of the operating points.

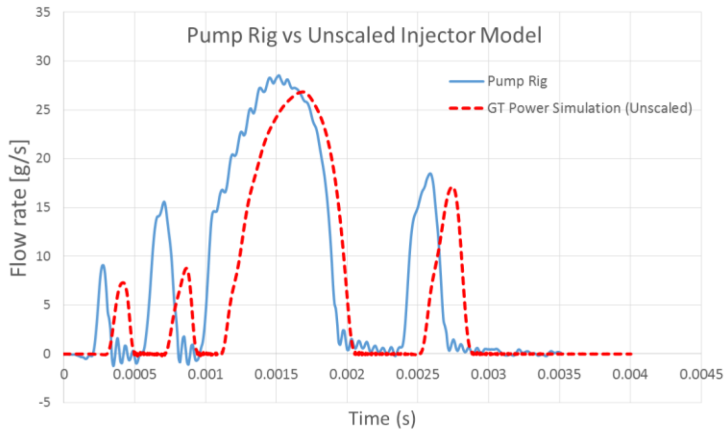

Figure 4.1: Injection rate profile of Predictive injector model vs Pump rig

It can be deduced from Figure 4.1 that the simulated rate profile from the GT-Suite injector model lacks in quantity, which is evident from the reduced area under the curve. The error in timing is attributed to the difference in hydraulic delay, which was around 190 μs in the test data and around 310 μs in the model. It is also important to note that the instantaneous slope at the start of each injection was much steeper for the measured data compared to the model. These factors can cause deviations in the critical parameters of the injected fuel packet at each time step such as mass of injected fuel per packet, velocity, breakup length, entrainment and subsequently the amount of fuel taking part in the combustion, as explained in section2.2.3.2. This would cause a deviation between the measured and predicted combustion parameters.

In order to overcome the inaccuracy in fuel quantity delivered, the rail pressure was iterated for each case until the test and simulated fuel quantity matched well. The ratio of scaled rail pressure to the base rail pressure was averaged for all the cases to arrive at a single scaling factor of 1.16, which could be applied for all the test cases. After scaling the rail pressure by this constant factor, the error in fuel quantity reduced significantly as shown in table 4.1. To compensate for the error in injection timing, the hydraulic delay in the GT-Suite model was adjusted. The rate profile for one of the cases after scaling the rail pressure and adjusting the hydraulic delay is shown in figure 4.2

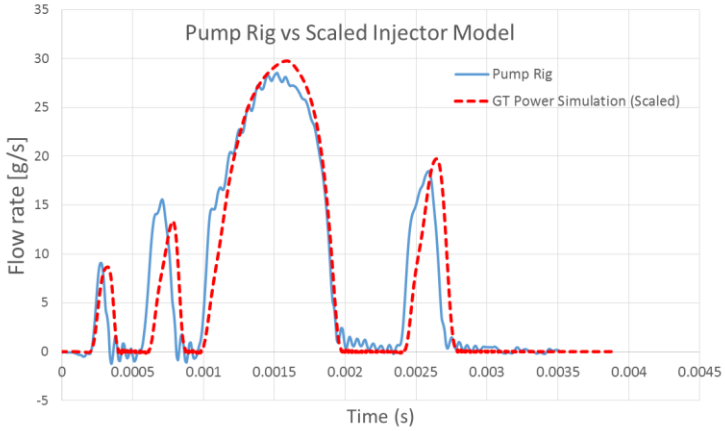

Figure 4.2: Injection rate profile (Scaled) of Predictive injector model vs Pump rig

Table 4.1: Error in fuel quantity before and after scaling the model

Sl no	Error in quantity before scaling (%)	Error in quantity after scaling (%)
1	-27.2	4.8
2	-26.7	3.3
3	-24.3	1.9
4	-30.1	-4.8
5	-27.9	-0.7

Although the error in fuel quantity and timing was reduced significantly after the corrections mentioned above, the error is still quite large and it was recommended by Gamma Technologies to not use this model for further calibration. Hence the Injector Rate Map (IRM) as described in section 3.3 was evaluated to address this error. The benefit of the IRM is that the fuel quantity desired per pulse and the start timing of each pulse can be entered by the user. This helps minimize the error in quantity and timing as can be seen in figure 4.3. However, there were still inaccuracies in the slope of rate profile, but it was better compared to predictive injector model. The IRM was used further for this thesis.

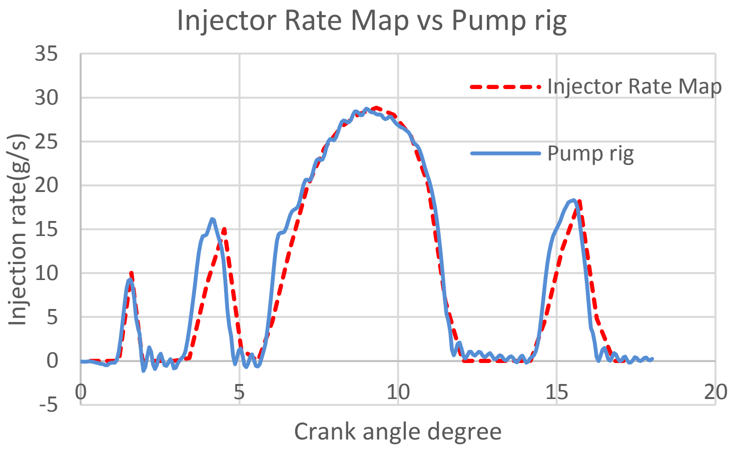

Figure 4.3: Injection rate profile of injector rate map vs pump rig

Since the IRM was populated using the predictive injector model, the rail pressure used in IRM was also scaled up by the same factor as in the predictive injector model (1.16). Although, unlike the predictive injector model the quantity per pulse and the injection start timing is not sensitive to the rail pressure, the rate profile is still sensitive. For example, a higher rail pressure will result in the same fuel mass injected in lesser time and would have an earlier End of Injection (EOI) compared to the case with a lower rail pressure. Figure 4.4 shows the variation of rate profile with rail pressure. Since a singular scaling factor for rail pressure was used for all cases to enable model scalability, it would not have been optimal for all cases and would have an impact on the combustion model calibration quality. The variation in the cylinder pressure trace against rail pressure can be seen in Figure 4.5. As the rail pressure increases, more fuel is available earlier during combustion and this increases the peak pressure. Similarly, this would also have an effect on other combustion and emission parameters. Hence this stands out to be one of the major reasons for any inaccuracies in the combustion model.

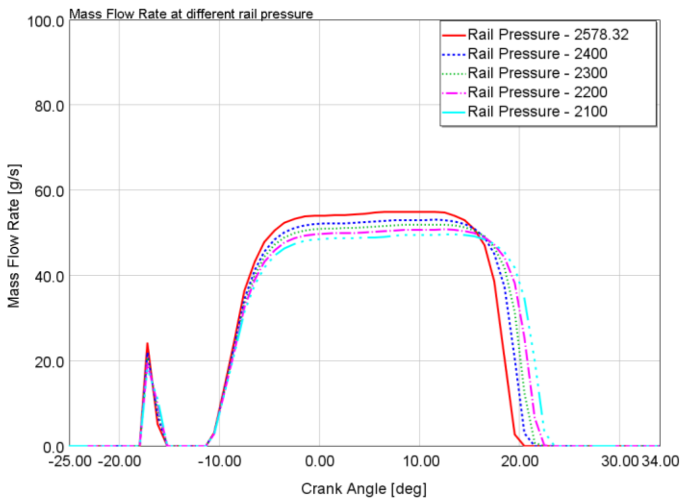

Figure 4.4: Variation in Injection profile and EOI at different rail pressure

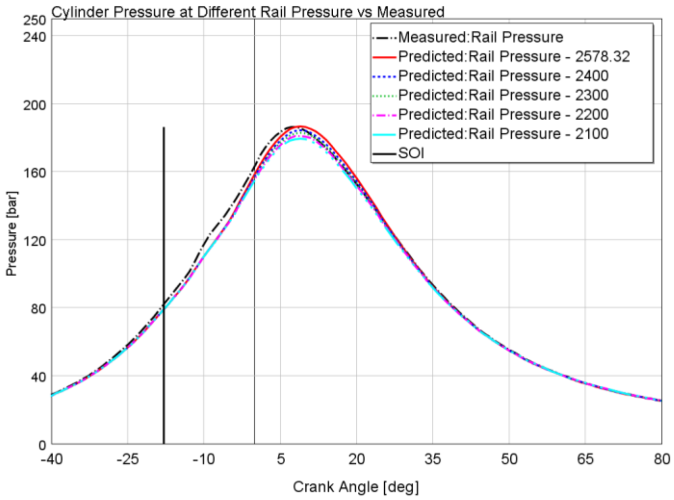

Figure 4.5: Variation in Predicted vs measured pressure at different rail pressure

4.2. TEST DATA VERIFICATION

As explained in section 2.3 there are three most common errors which can occur during the measurement of cylinder pressure in a test cell. These are namely encoder error, pegging error and error due to thermal shock. The procedure for identifying if these errors exists have been explained in section 3.2.

- **Encoder error**
  The motored cylinder pressure trace was analyzed and the peak pressure was found to occur at 0.9 CAD before TDC, which is within the recommended limit of 1 CAD. However, it should be noted that this check does not guarantee that the encoder error does not exist. The best option would be to use a TDC sensor as explained in section 2.3.1 unfortunately, this was not available in the test cell at Volvo Cars.

- **Pegging error**
  The polytropic coeffcient for all the cases was found to be close to the recommended range of 1.35 – 1.37, as shown in figure 4.6, which is typical for DI Diesel engines.

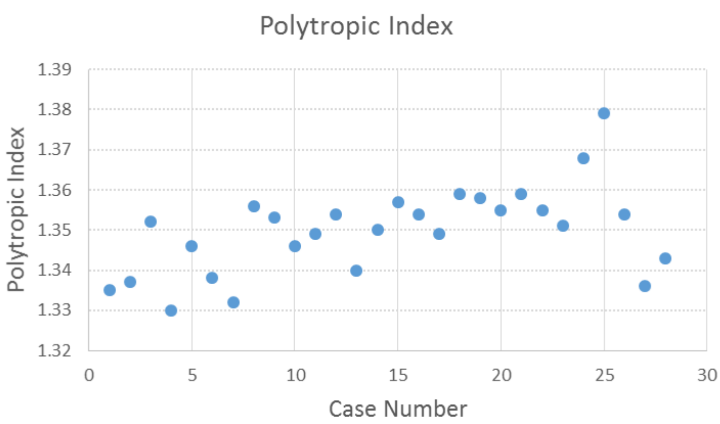

Figure 4.6: Polytropic Index for all the cases

In AVL Concerto the the dispalcment volume is not compensated for with changes in compression ratio. Hence, when the compression ratio is changed from the geometric value to the dynamic value, the polytropic coeffecient calculated may not be accurate. Therefore, although the polytropic coeffecients are not excalty within the recommnded range, the intention was to see that there were no unreasonable values (less than 1.30 or greater than 1.40) during the compression stroke (-90 to -40 degrees BFTDC), which is unrepresentative of a DI Diesel engine.

The pressure diffrence between the cylinder pressure at intake BDC and intake pressure at ± 5 CAD of intake BDC was found to be within the recommended limit of 200 milli bar as mentioned is section **3.2.2** for all cases. A higher pressure shift on either side might point to an error in the input data with respect to pressure referencing. The impacted parameter due to incorrect pegging would be peak pressure and polytropic coefficient during compression.

- **Thermal shock**
  The average exhaust absolute pressure was calculated for all the cases and was found to be within the recommended limit of 4kPa. The window for measurement between 240 to 320 CAD after firing TDC as mentioned in section 3.2.3 is only a general recommended value. Even if the standard deviation exceeds this value in the specified window, the pressure trace may still recover before the pegging point (intake BDC) in the next cycle. Hence it is recommended to include the point for TPA analysis and check for any unusual heat release tail, which can be indicative of the presence of thermal shock in the measurement data.

4.3 THREE PRESSURE ANALYSIS (TPA)

The TPA was performed on all 28 points and the following results were observed.

1. **Pressure trace matching**
   The simulated pressure trace was visually verified and found to match well with the measured pressure trace for all 28 points. Figure 4.7 shows the pressure trace of one of the best and worst matching cases.

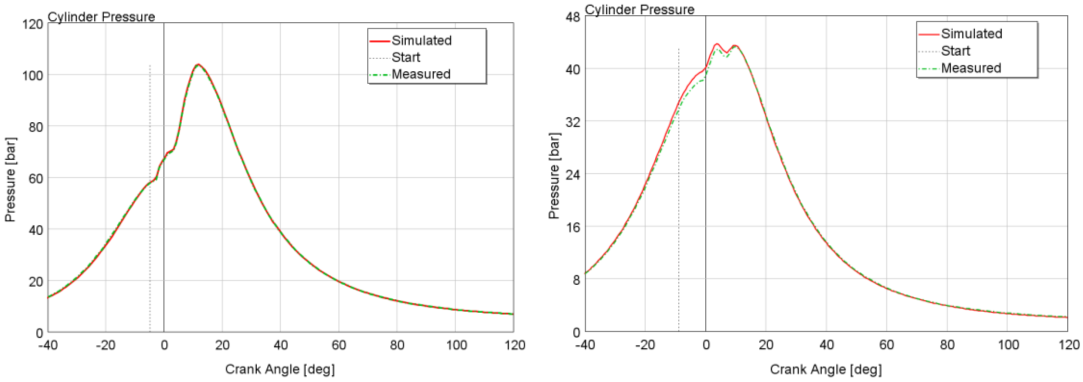

Figure 4.7: Measured vs. simulated pressure trace in TPA for the best and worst matching cases

As mentioned in section 3.4.1, initially during the TPA analysis the compression ratio was manually varied until the pressure trace between measured and simulated matched well. However, to facilitate model scalability an average compression ratio for all points was calculated and found to be 15.1. The TPA was re-run for all points with this average compression ratio. Due to this, in some of the cases the deviation in pressure trace was larger than in others as shown in figure 4.7.

2. **Consistency checks.**

As explained in section 3.4, GT-Power does a series of consistency checks to validate the quality of data. The results of the consistency checks are shown in table 4.2.

Table 4.2: Consistency check summary for TPA analysis

Error Type	Number of Cases
Pressure Smoothing	15
Cumulative Burn During Compression	1
Fraction of Fuel Injected Late	3
Large Change in LHV required	3

However, a failure in one of the consistency checks does not mean that the case should be rejected for DI-Pulse calibration. It is up to the users to decide the impact of the error on the final calibrated model and whether to include the point for calibration.

For most of the cases the pressure smoothing error was reported. However, visually the pressure and burn rate profile were found to be reasonably smooth without traces of noise. Hence the error was ignored after further consultation with Gamma Technologies.

Error in cumulative burn during compression was reported in a single case. In this case the change in compression ratio after using the average compression ratio was the largest compared to all the other cases. This led to a higher deviation in the simulated compression curve compared to the measured, which led to a positive burn rate before the actual SOI.

Error in Fraction of fuel injected late was mainly because of using a single scaling factor for injection rail pressure in the IRM as discussed in section 4.1.

The LHV multiplier error indicates an error with the input data such as measured pressure, injection profile, etc. Since the errors were very close to suggested deviations of 5%, it was neglected after consulting with Gamma technologies.

Therefore, despite the errors in consistency checks all 28 points were found to acceptable and was used further in this thesis.

3. **IMEP variation**

The variation between the measured and simulated IMEP for each point was calculated and plotted as shown in figure 4.8. The IMEP variation was found to be within the recommended limit of ± 5%.

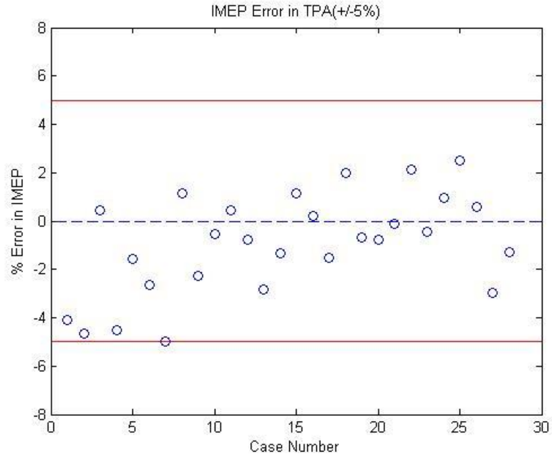

Figure 4.8: IMEP % error of TPA vs measured data

4.3.1 TPA ANALYSIS WITH PREDICTIVE INJECTOR MODEL

As an additional validation, the predictive injector model without any scaling was used to perform the TPA on 10 randomly picked points out of the 28 points. All the cases reported an error in fuel mass and LHV multiplier with values well beyond the recommended error limit. The pressure trace also did not match well. A comparison of the simulated vs measured pressure trace using an injector rate map and a predictive injector model is shown figure 4.9. This result was expected since the injector model consistently delivers less fuel compared to the flow rig data.

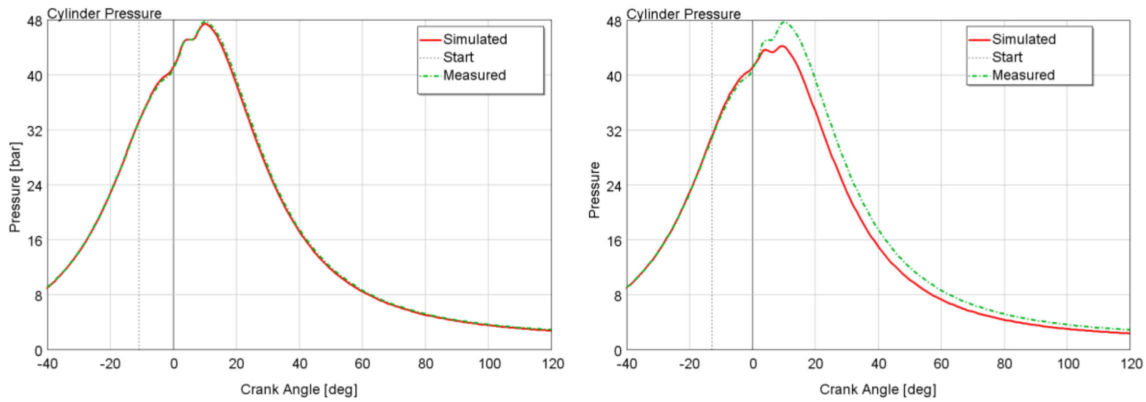

Figure 4.9: Measured vs simulated pressure trace using an IRM and injector model (unscaled)

4.4 CYLINDER PRESSURE ONLY ANALYSIS

The CPOA was performed on all 28 points and the following results were observed.

1. **Pressure trace matching.**
   The simulated and measured pressure trace was verified visually and found to match well for all 28 points. Figure 4.10 shows the pressure trace of the same cases shown in TPA in figure 4.7.

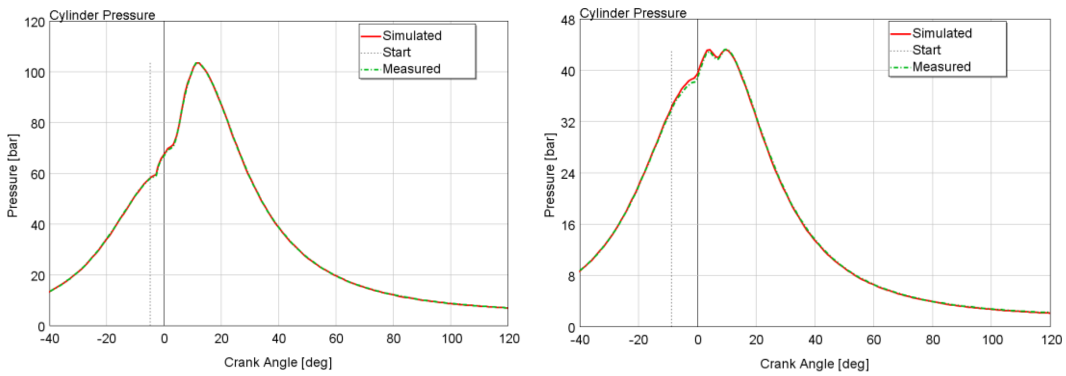

Figure 4.10: Measured vs. simulated pressure trace in CPOA for the same cases shown in TPA (fig 3.4)

2. **Consistency checks.**
   The table below shows the results of the consistency checks described in section 3.4.

Table 4.3: Consistency check summary for CPOA analysis

Error Type	Number of Cases
Pressure Smoothing	14
Cumulative Burn During Compression	1
Fraction of Fuel Injected Late	2
Large Change in LHV required	0

The number of cases with pressure smoothing error and cumulative burn duration remains the same as in TPA. However, it is interesting to note that none of the cases reported error in large LHV change required, while the error in fraction of fuel injected late reduced by 1 compared to TPA. This can be explained by the fact that, CPOA is a closed volume analysis as mentioned in section 2.4 hence the results are based only on the trapped quantities at IVC. So it is possible that the consistency check errors might change from TPA to CPOA. However, for the same reasons mentioned in the case of consistency check errors in TPA, all the 28 points were valid and used for further work in this thesis.

3. **IMEP Variation.**
The variation between the measured and simulated IMEP was calculated and plotted as shown in figure 4.11. The IMEP variation was found to be within the recommended limit of ± 5%.

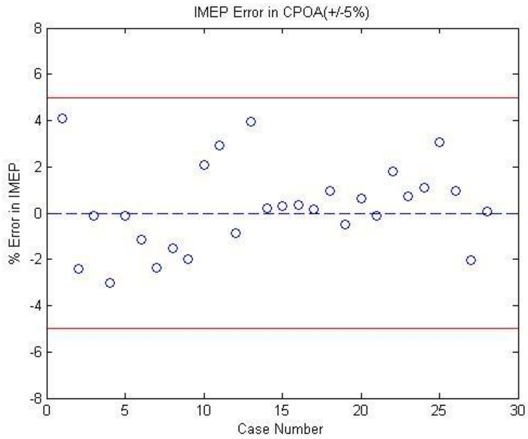

Figure 4.11: IMEP % error of CPOA vs measured data

4.5 DI-PULSE CALIBRATION

The DI-Pulse calibration was performed for 25 points and 3 points were reserved for validation of the model as shown in Fig 3.2. Fig 4.12 and 4.13 shows the results of the pressure trace and burn rate from the calibrated model for the best and worst cases.

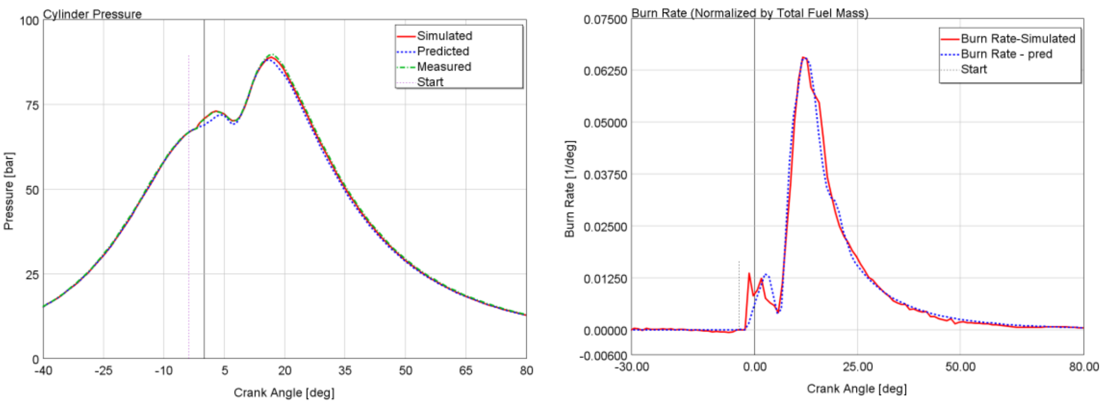

Figure 4.12: Pressure and Burn rate plots of one of the well calibrated points.

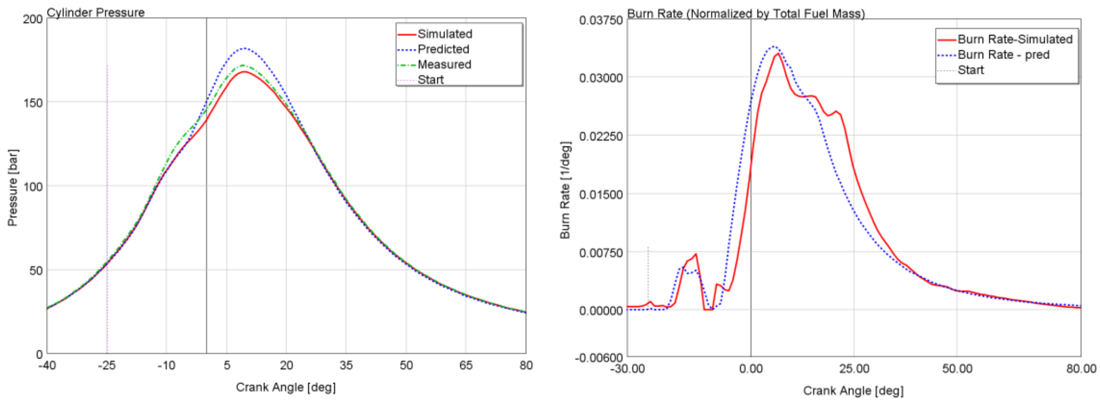

Figure 4.13: Pressure and Burn rate plots of one of the not well calibrated points.

In general, the predicted and measured pressure trace and burn rate matched well for most of the low to mid speed and low to mid load operating points while, the points in the high speed and high load region did not match as well. The possible reason for this is that most of the points used in the calibration were in the low to mid speed and low to mid load region. Hence the multipliers obtained for the combustion model may have been more representative for these points. Also, it is believed that the rail pressure scaling factor used for the IRM may not be optimal for these high speed and high load points, which could have also contributed to the error. However, despite the deviations all the average RLT (result) parameters were found to be within the recommended error limit except for NO_x which is slightly outside the limits as shown in table 4.4.

Table 4.4: Average error for 25 points used for calibration

Parameter	Unit	Average Error Limit	Average Error Calculated
Burn rate	rms	0.0054	0.0045
IMEP	%	2.2	1.66
CA50	Degree	0.9	.83
Max. Pressure	Bar	2.8	2.56
NO_x (ppm)	%	20	20.88

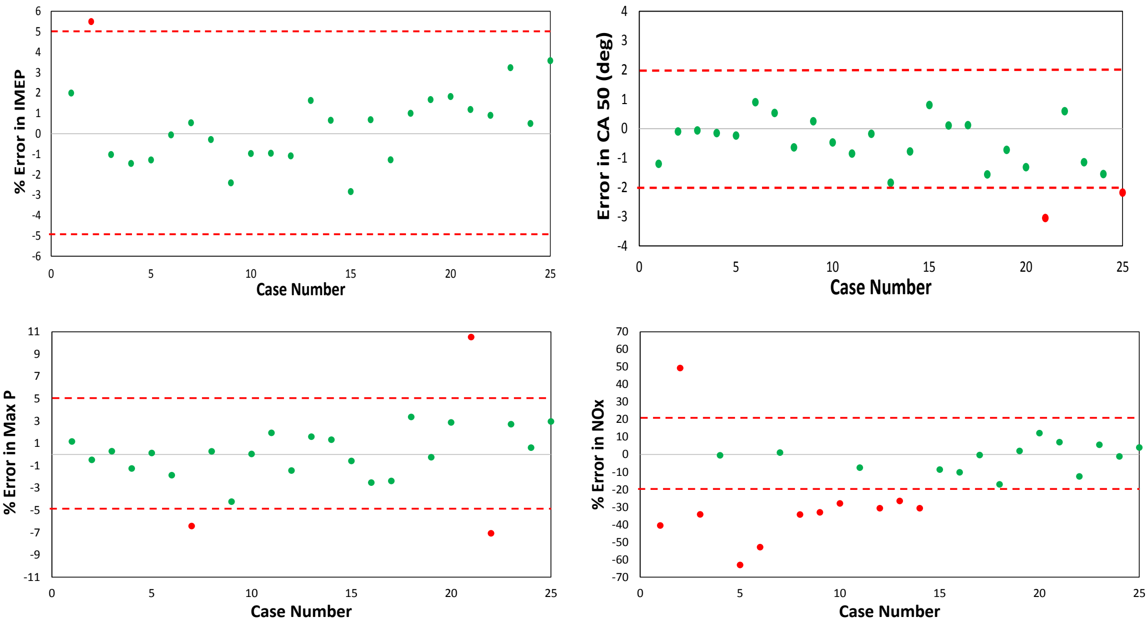

Figure 4.14: RLT errors after calibration of DI-Pulse model (IMEP error, CA50 error, Max cylinder pressure error and NO_x)

The instantaneous RLT error plots for all points are shown in figure 4.14. It can be seen that the instantaneous error for most points are within the range for all parameter except NO_x.

Cases 20 to 25 represent the high speed and high load operating points. The errors in these points are significantly higher compared to the other points except for NO_x. The NO_x error trend is opposite compared to the other parameters. The prediction is very good at mid to high speed and mid to high load points (Case 15 –Case 25) while, it is not so good at the low speed and low load points (Case 1- Case14). It is quite hard to exactly state the reason for the deviation in NO_x predictions, it could probably be because of the model limitation. Since NO_x formation is strongly dependent on the local temperatures and the model may not be able to capture this effect

Although the error percentage for NO_x is outside the limits a closer examination on the absolute values indicate that the NO_x predictions follow the trend of measured NO_x values quite well as shown in figure 4.15. Hence the model can still be used for a trend analysis of NO_x.

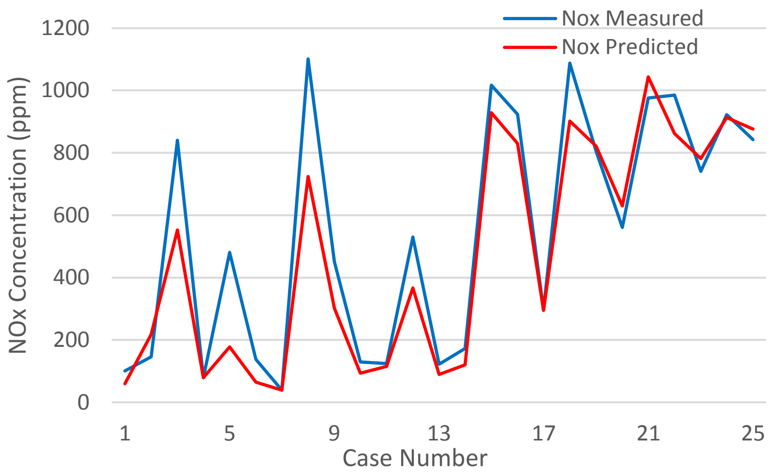

Figure 4.15: Measured vs predicted NOx concentration in ppm

4.6 DI-PULSE PREDICTION

As mentioned in section 3.9 the ability of the calibrated DI-Pulse model to predict the combustion characteristics was tested on 3 points, one each at low, mid and high load region at different speeds as shown in figure 4.16.

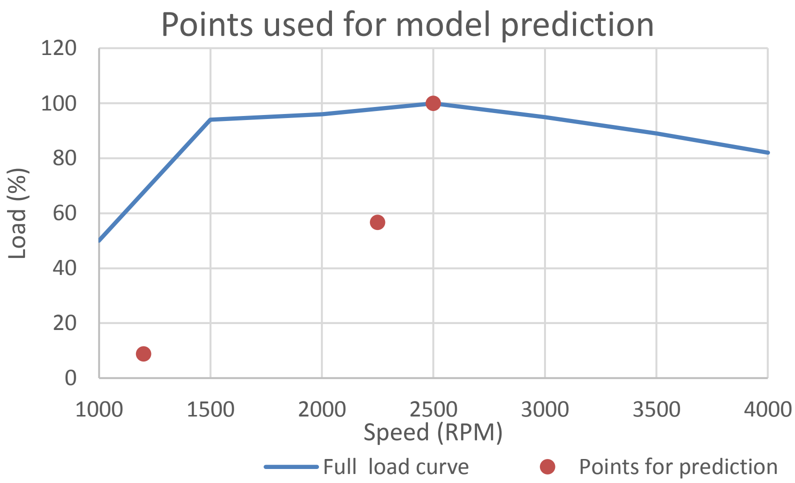

Fig 4.16: Plot of points used for testing DI-Pulse model prediction

The instantaneous RLT (result) variables were compared against the error limit recommended by Gamma Technologies and the results are tabulated in table 4.5. The absolute values of these parameters are shown in table 4.6. The NO_x error exceeds the limit significantly for the low load point and maximum pressure error exceeds the limit in the high load point. Both these errors follow the trend seen in the DI-Pulse calibration result explained in section 4.5. The measured vs. predicted burn rate and pressure trace plots for these 3 points is shown in figure 4.17, 4.18 and 4.19. Visually the plots look quite good except for the burn rate plot at the low load point. Nevertheless, on observing the RMS error in burn rate for this point as shown in table 4.5 the deviation is well within the limit. In general the predictive capability of the model is quite good.

Table 4.5: Average error for 3 points used for validation

Parameter	Unit	Error Limit	Low load	Mid load	High load
Burn Rate Error	RMS	.0052	0.011	.002	.0026
IMEP	%	+/-5	1.75	-0.45	-0.69
CA50	Degree	+/-2	0.1	-1	1
Max. Pressure	Bar	+/-5	0.9	3.4	-6.7
NO_x (ppm)	%	+/-20	-34.3	5.7	-17.1

Table 4.6: Absolute value of the predicted variables for the 3 validation points

Operating Point	CA50% (Meas.) [CAD]	CA50% (Pred.) [CAD]	Max Pressure [bar]	Max Pressure [bar]	NO_x (Meas.) [ppm]	NO_x (Pred.) [ppm]
Low load	9.6	9.7	43.2	44.1	79.7	52.4
Mid load	15.1	14.1	114.9	118.3	274.7	290.5
High load	16.1	17.1	173.2	166.5	1087.5	902.03

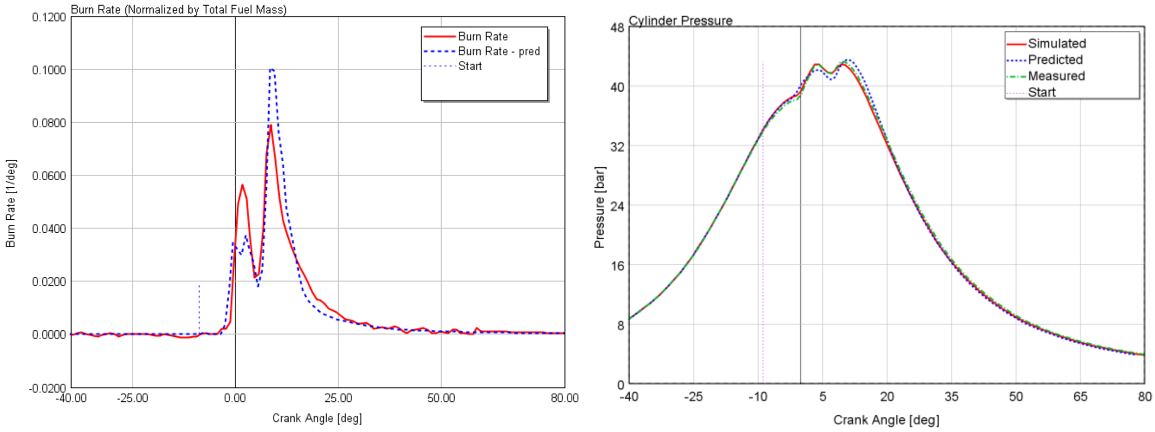

Figure 4.17: Low load point, Predicted pressure and burn rate

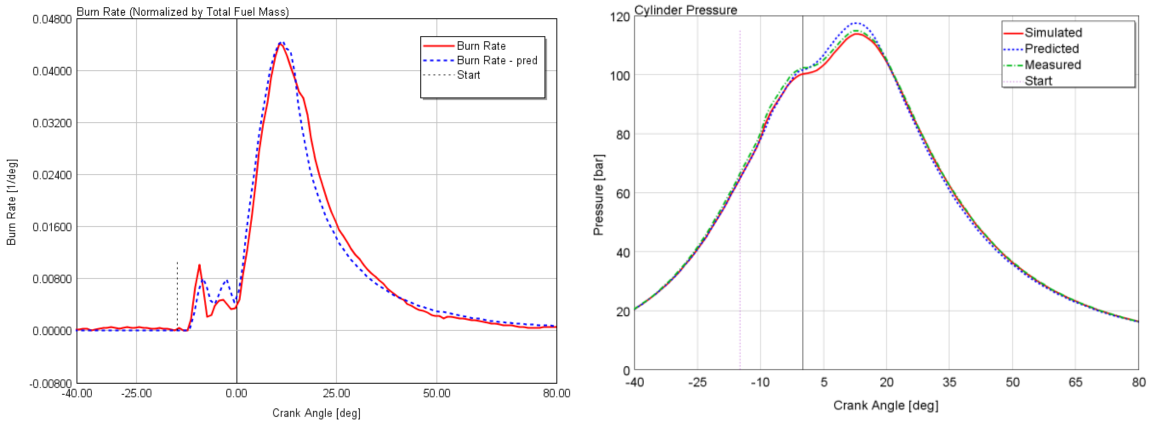

Figure 4.18: Mid load point, Predicted pressure and burn rate

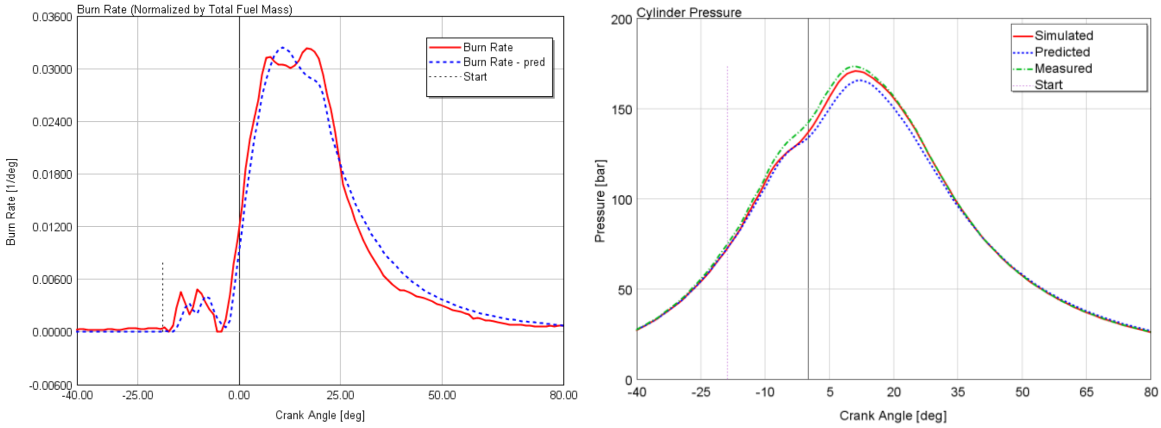

Figure 4.19: High load point, Predicted pressure and burn rate

5 CONCLUSION

Test was conducted for 28 operating points obtained from the RDE cycle at Volvo Cars. These points provided a good spread of key operating variables such as EGR, injection strategy and swirl. Preliminary checks for the test data was done in AVL Concerto and none of the points had any errors. After the preliminary verifications, three pressure analysis was performed on the data and trapped quantities were obtained. The test cell data was also validated using the TPA and found to be satisfactory. Subsequently, CPOA analysis was performed and the accuracy of the trapped quantities obtained from TPA analysis was validated and found to be acceptable.

The injector model forms a critical part in the accuracy of the DI-Pulse calibration model. There were two options available, either to use the detailed injector model or the injector rate map. The detailed injector model was found to be inaccurate both in terms of fuel quantity and timing even after scaling the commanded rail pressure and compensating for the hydraulic delay. This led to the evaluation of the injector rate map, which was populated using the detailed injector model. It showed good conformance with the test data obtained from the injector flow bench in terms of both injection timing and fuel quantity delivered. This combined with the fast execution time and model scalability made it the appropriate choice for fuel injection input in this thesis.

After data validation, the DI-Pulse calibration was carried out for 25 operating points. The results were considerably better for low to mid load and low to mid speed operating points compared to the high load and high speed operating points. This could be due to the fact that more number of points used in the calibration was spread in this region. The other probable cause could be the reduced accuracy of the IRM in the high load and high speed region as explained in section 4.1. Nonetheless, the average error of all the RLT (result) parameters except NO_x was found to be well within the limit prescribed by Gamma Technologies. The average error in NO_x was 20.9% while the limit is 20%. It was interesting to note that the NO_x prediction was particularly poor at low load and low speed where the EGR content is quite high, while at mid to high load and mid to high speed the predictions were good. The exact reason for this trend is hard to pin point but it could be a model limitation. Nevertheless, the model predicts the NO_x trend quite well and can be used for trend analysis.

Finally the DI-Pulse model was validated against 3 points, one each at low load-low speed, mid load-mid speed and maximum torque point. The error in all the RLT parameters was within the limits except for maximum pressure in the max. torque point and NO_x in the low load point. These deviations could be due to the same reason mentioned above for the calibration.

To sum up, the base model provides good prediction capabilities throughout the entire map for the key RLT parameters, except for NO_x in the region with high EGR percentage. However, the trend of NO_x predictions was found to be good throughout the operating points tested.

6 RECOMMENDATION AND FUTURE WORK

This section describes briefly about the recommendations made to Volvo Cars and Gamma Technologies and the future work that could be carried out in different sections including the test cell, AVL Concerto, the engine and injector model in GT-Suite and the DI-Pulse model, in order to further improve the quality of the combustion model and calibration process.

6.1 TEST CELL

The phasing of $P - \theta$, strongly governs the output of heat release analysis. The current method to obtain the encoder error using a motoring curve is a coarse validation as explained in section 3.2.1. Therefore the use of a TDC sensor is recommended for future combustion model calibration work, as it provides the best accuracy for encoder error detection.

6.2 AVL CONCERTO

The heat release analysis script in Concerto lacks a heat transfer model. This results in a negative heat release before the actual start of injection (SOI). This can be confusing to some users. Hence it is recommended to add and tune a heat transfer model (ex. Woschni), to improve the overall quality of the preliminary analysis.

It is advised to turn off the pressure correction feature in Concerto. Since the displacement volume is not compensated for in the pressure correction script with changes in the compression ratio. Another limitation is that the load varying compression ratio can’t be captured in the test cell. This means that the polytropic exponent obtained from Concerto is not entirely accurate and should only be used to verify if it is close to the realistic range (1.35 – 1.37). The recommended option is to feed the raw pressure data directly to GT-Power, and perform the compression ratio matching. The resultant polytropic exponent should be taken as the baseline.

As described in section 3.2, the thresholds for the data quality checks are general guidelines and in no case it should be used as a base for rejection of data. It is always recommended to perform the TPA and CPOA analysis to ascertain the final data quality.

6.3 ENGINE MODEL

The engine model used for three pressure analysis lacked the capability to simulate the effect of valve dynamics. This led to tuning of the gas exchange as explained in section 3.4.2 to improve the quality of analysis. Hence it is recommended to include a calibrated valve model incorporating valve dynamics to improve the quality of results and minimize the gas exchange tuning which can be a time consuming process. It is also recommended to explore the usage of a blow-by model in GT-Power. If such a model can be conceived, then the user can reduce the time spent in the adjustment of compression ratio as explained in section 3.4.1

The best case scenario is an integrated engine-injector model in terms of future research and model scalability. The initial trial to conceive such a model resulted in very high runtime. It is recommended to work together with the injector supplier and Gamma Technologies to investigate the problem further.

6.4 INJECTOR MODEL

The currently available injector model was found to be significantly inaccurate in terms of both timing and quality. Based on the initial investigation, following approaches are recommended

- It is strongly recommended to get an updated GT-Suite injector model from the supplier, or from a third party. Further the model should be validated against reliable test data obtained from flow bench tests and used with integrated engine model. This method is recommended by Gamma Technologies.

- Injector rate map is a great choice from model scalability and runtime aspects. The performance of injector rate map should be validated against a variety of different injection strategies and rail pressure before being used in the TPA and DI-Pulse model.

- It should be investigated if it is possible to accurately measure the rate profile in the engine test cell directly. This would be useful as the injector flow would be most accurately represented with respect to operating conditions (e.g. complete fuel rail, backpressure, temperature, etc.).

- Finally, it is also possible to use the data measured from injector flow bench directly. This method is not recommended as it may have signal noise, which needs to be filtered. Also from scalability aspects this approach is poor as the pump rig needs to be readily available whenever a new point has to be included in the model.

6.5 DI PULSE CALIBRATION AND VALIDATION

The multipliers obtained from the DI-Pulse combustion multipliers optimization algorithm provided by Gamma Technologies should not be considered as final. Efforts can be made on the part of the user to manually fine tune the values because the algorithm works primarily on minimizing only the burn rate error. It is recommended to investigate with Gamma Technologies if they can incorporate other variables of interest such as – Max pressure, IMEP percentage error and CA 50% burn as objective functions for optimization. This would help reach a more optimized result quickly.

Gamma Technologies recommends between 25-200 points for the calibration of the model. In this thesis only 25 points were used due to time constraint. If additional points are to be chosen for calibration there are two ways to do this. Either choose more points at the low-mid load and low-mid speed region by performing sweeps of EGR and swirl at fixed operating points or choose additional points at the high load and high speed region. The reason for recommending to take sweeps of EGR and swirl at low-mid load and low-mid speed region is that they have a strong influence on the combustion characteristics. However, since the current model predicts the combustion well at these regions compared to the high load and high speed region, it is strongly recommended to choose the latter option first.

For the purpose of model validation, only three points were evaluated, which is not an ideal way to validate the model. Including more points for validation was not possible due to time constraints. So, it is suggested to conduct a sensitivity analysis of the model by performing sweeps of EGR, injection timing and swirl at fixed operating points. Only after obtaining these results can a sound decision be made about the model’s capabilities.

6.6 DI-PULSE NO_x MODEL

The current DI-Pulse model can only predict NO. While a significant amount of NO_2 is found in the emissions particularly at low loads. Hence it is recommend to Gamma Technologies to further investigate and model the NO_2 emissions.

The NO predictions using this model was found to be poor particularly at low loads and low speeds. The exact reason for this is hard to pin point but the most probable cause is the model limitation. It is recommended to discuss with Gamma Technologies about how to further improve the model.

7 REFERENCES

7.1 REFERENCES TO TEXT

Asad, U., Zheng, M., Han, X., T. Reader, G. and Wang, M. (2008). Fuel Injection Strategies to Improve Emissions and Efficiency of High Compression Ratio Diesel Engines. SAE International.

AVL, (2015). AVL Concerto combustion measurement. [Online] Available at: https://www.avl.com/-/avl-concerto-data-post-processing

Badami, M., Mallamo, F., Millo, F. and E E., R. (2002). Influence of Multiple Injection Strategies on Emissions, Combustion Noise and BSFC of a DI Common Rail Diesel Engine. SAE International.

Barba, C., Burkhardt, C., Boulouchos, K., & Bargende, M. (2000). A Phenomenological Combustion Model For Heat Release Rate Prediction In High-Speed DI Diesel Engines With Common Rail Injection.

CarsDirect, (2015). Diesel Fuel vs. Unleaded Gasoline. [Online] Available at: http://www.carsdirect.com/car-buying/diesel-fuel-vs-unleaded-gasoline-understand-the-pros-and-cons.

Colin, O., Benkenida, A. and Angelberger, C. (2003). 3D Modeling of Mixing, Ignition and Combustion Phenomena in Highly Stratified Gasoline Engines. Oil & Gas Science and Technology, 58(1), pp.47-62.

Davis and Patterson (2006). Cylinder Pressure Data Quality Checks and Procedures to Maximize Data Accuracy. SAE International.

Diesel net, (2013). Denso announces 2500 bar common rail injection system. [online] Available at: https://www.dieselnet.com/news/2013/06denso.php

Environment Portection Agency,USA (2015). Nitrogen dioxide. [Online] Available at: http://www.epa.gov/oaqps001/nitrogenoxides/health.html

GT- SUITE(2013), Engine Performance Application Manual, v 7.4

Gtisoft.com, (2015). Applications. [Online] Available at: http://www.gtisoft.com/applications/a_Engine_Performance.php.

Günter, Merker, Schwarz, Christian, Teichmann, Rüdiger (2012). Combustion Engines Development. Springer.

Heywood, J. (1988). Internal combustion engine fundamentals. New York: McGraw-Hill.

Hountalas, D., Lamaris, V., & Pariotis, E. (2010). Identification of the Error Introduced in DI Diesel. SAE International, (2010-01-0153), pg.4-5

J, O. (2014). Denso injector GT suite model operation manual.

Jung, D. and N. Assanis, D. (2001). Multi-Zone DI Diesel Spray Combustion Model for Cycle. SAE International.

K. Khair, M. and Jääskeläinen, H. (2014). Exhaust Gas Recirculation. [online] Diesel net. Available at: https://www.dieselnet.com/tech/engine_egr.php

.

Kitchen, T. (2015). Common Rail Diesel Fuel System. [online] Available at: https://personel.omu.edu.tr/docs/ders_dokumanlari/894_52413_1913.pdf.

Klein, M. (2004). A specific heat ratio model and compression ratio estimation. Linkoping: Univ.

Lancefield, T., Methley, I., Räse, U. and Kuhn, T. (2000). The Application of Variable Event Valve Timing to a Modern Diesel Engine. SAE International.

Li, P., Zhang, Y., Li, T. and Xie, L. (2015). Elimination of fuel pressure fluctuation and multi-injection fuel mass deviation of high pressure common-rail fuel injection system. Chinese Journal of Mechanical Engineering.

Livengood, J., Wu, P. (1955). Correlation of autoignition phenomena in internal combustion engines and rapid compression machines. Symposium (International) On Combustion, 5(1), pp. 347-356.

Mark Bos. (2007), Validation GT-Power Model Cyclops Heavy Duty Diesel Engine. TU Eindhoven. [online]. Available at:http://w3.wtb.tue.nl/fileadmin/wtb/ct-pdfs/Master_Theses/eindverslag_Mark%20Bos.pdf

Maurya, Datt Pal, Agarwal (2013). Digital signal processing of cylinder pressure data for combustion diagnostics of HCCI engine. Elsevier Journal.

Ohlsson, J. and Sonander, J. (2015). Evaluation of the DI-Jet combustion model with an integrated fuel injection system.

Patil, S. (2012). Investigation on Effect of Variation in Compression Ratio on. [online] Available at: https://globaljournals.org/GJRE_Volume12/1-Investigation-on-Effect-of-Variation.pdf.

Payri, F., Olmeda, P., Martin, J., & Garcia, A. (2011). A complete 0D thermodynamic predictive model for direct injection diesel engines. Applied Energy, 88(12), pp. 4632-4641.

Rajput, R. (2007). Internal combustion engines. Bangalore, India: Laxmi Publications, pp.226-230.

REIFARTH, S. (2010). EGR-Systems for Diesel Engines. KTH thesis.

Robert Wang, (2014). Predictive Combustion Modeling. Gamma Technologies

Rosli, N. (2011). Effects of split injection and exhaust gas recirculation strategies on combustion and emissions characteristics in a modern V6 diesel engine. Phd thesis University of Birmingham.

Schäfer, F. and Van Basshuysen, R. (1995). Reduced emissions and fuel consumption automobile engines. Wien: Springer-Verlag.

Sharma, B. (2014). Air Pollution. Krishna's, pp.336-350.

Southernfs, (2015). Soot in Diesel engines. [online] Available at: http://www.southernfs.com/energy/Documents/Soot%20in%20Diesel%20Engines.pdf

Sundararajan (2015). Gas Power cycles. [online] NPTEL IIT Madras. Available at: nptel.ac.in/courses/IIT-MADRAS/Applied_Thermodynamics/Module_4/6_Asdc.pdf

Taylor, C. (1966). The internal-combustion engine in theory and practice. Cambridge, Mass.: M.I.T. Press, p.33. .

Zhao, H. (2010). Advanced direct injection combustion engine technologies and development. Boca Raton: CRC Press, p.223.

7.2 REFERENCE FOR FIGURES

Asad, U., Zheng, M., Han, X., T. Reader, G. and Wang, M. (2008). Fuel Injection Strategies to Improve Emissions and Efficiency of High Compression Ratio Diesel Engines. SAE International.

Denso (2015), GT Suite Injector mode provided to Volvo Cars.

E. Dec, J. (1997). A Conceptual Model of DI Diesel Combustion Based on Laser Sheet Imaging. SAE Paper.

GT-SUITE(2013), Engine Performance Application Manual, v 7.4.

George Anitescu(2012), Green Car Congress. [Online] Available at http://www.greencarcongress.com/2012/05/anitescu-20120504.html

H.Hiroyasu, T.Kadota, M.Arai (1983), Development and use of a spray combustion modelling to predict diesel engine efficiency and pollutant emissions. Bulletin of JSME 01/1983.

K. Khair, M. and Jääskeläinen, H. (2014). Exhaust Gas Recirculation. [online] Diesel net. Available at: https://www.dieselnet.com/tech/engine_egr.php

Kitchen, T. (2015). Common Rail Diesel Fuel System. [online] Available at: https://personel.omu.edu.tr/docs/ders_dokumanlari/894_52413_1913.pdf.

Maurya, Rakesh Kumar, and Avinash Kumar Agarwal. 'Investigations On The Effect Of Measurement Errors On Estimated Combustion And Performance Parameters In HCCI Combustion Engine Measurement 46.1 (2013): 80-88. Web.

REIFARTH, S. (2010). EGR-Systems for Diesel Engines. KTH Thesis.

Soloiu, V. (2013). Investigation of Low Temperature Combustion Regimes of Biodiesel With N-Butanol Injected in the Intake Manifold of a Compression Ignition Engine. ASME.